Russian Geology and Geophysics © 2022, Novosibirsk State University
Vol. 63, No. 4, pp. 435–457, 2022 *DOI:10.2113/RGG20214425* *Geologiya i Geofizika*

Epithermal Au–Ag–Se–Te Deposits of the Chukchi Peninsula (Arctic Zone of Russia): Metallogeny, Mineral Assemblages, and Fluid Regime

N.S. Bortnikov[a], A.V. Volkov[a, ✉], N.E. Savva[b], V.Yu. Prokofiev[a], E.E. Kolova[b], A.A. Dolomanova-Topol'[a], A.L. Galyamov[a], K.Yu. Murashov[a]

[a]*Institute of Geology of Ore Deposits, Petrography, Mineralogy and Geochemistry, Russian Academy of Sciences, Staromonetnyi per. 35, Moscow, 119017, Russia*

[b]*N.A. Shilo Northeastern Interdisciplinary Research Institute, Far Eastern Branch of the Russian Academy of Sciences, ul. Portovaya 16, Magadan, 685010, Russia*

Received 14 September 2021; accepted 8 October 2021

Abstract—Numerous epithermal Au–Ag deposits and ore occurrences of the Chukchi Peninsula are localized in the Cretaceous Okhotsk–Chukotka (OCVB) continent-marginal and Late Jurassic–Early Cretaceous Oloi (OVB) island arc volcanic belts and in Early Cretaceous postcollisional volcanic troughs. Volcanotectonic depressions, calderas, and volcanic domes control the location of the deposits. The orebodies of the deposits are quartz–adularia veins, sometimes en-echelon ones forming extending vein zones, as well as isometric and linear stockworks. The auriferous veins of most deposits display complex breccia–crustification structures. The vein ores have rhythmically and colloform–banded structures, with a predominantly fine distribution of ore mineral grains, often with banded clusters of ore minerals (ginguro). Native gold is of low fineness; the dispersion of this index varies from low to high. Acanthite is widespread in the ores. Its highest contents are specific to deposits with the repeated redistribution of substance (Kupol, Corrida, and Valunistoe). Based on the results of mineralogical studies, most of the epithermal Au–Ag deposits of the Chukchi Peninsula can be assigned to the Se type. The ores of some deposits (Valunistoe, Dvoinoe, etc.) contain both Se and Te minerals. The telluride-richest sites of the Sentyabr'skoe and Televeem deposits are far from the main orebodies. Most of the Chukchi epithermal Au–Ag deposits have many common characteristics (low and moderate temperatures of fluids, low fluid salinity, domination of carbon dioxide over methane, etc.) typical of low-sulfidation deposits. The maximum temperatures and salinity are specific to fluids in the Central Chukchi sector of the OCVB and in the Baimka zone of the OVB, and the minimum ones are typical of fluids in the East Chukchi flank zone and inner zone of the OCVB. The average salinity of mineral-forming fluids in the inner zone of the OCVB is half as high as the salinity of fluids in the East Chukchi flank zone of this belt, although the sulfate content is higher. At the same time, the fluids in the inner zone of the OCVB are richer in carbon dioxide and bicarbonate ion than the fluids in the East Chukchi flank zone of this belt. The fluid inclusion data permit the Vesennee deposit (Baimka zone) to be regarded as an intermediate-sulfidation one and suggest the presence of epithermal high-sulfidation deposits in the inner zone of the OCVB.

Keywords: Arctic zone; epithermal Au–Ag deposits; mineralogical features; selenides; tellurides; fluid inclusions; thermobarogeochemistry; ore formation; Chukchi Peninsula

INTRODUCTION

The term "epithermal" was introduced by the famous American geologist W. Lindgren (Lindgren, 1933) and refers to near-surface (depth of <1 km) low-temperature hydrothermal occurrences of precious metals, related mainly to subaerial volcanism and, sometimes, volcanic products.

According to the generally accepted classification (White and Hedenquist, 1995), epithermal deposits are divided into two classes depending on the oxidation state of sulfur in hydrothermal solutions: low-sulfidation (LS) and high-sulfidation (HS) ones. Later, one more class, intermediate sulfidation (IS), was recognized (Hedenquist et al., 2000). The LS deposits are usually characterized by the presence of pyrite–pyrrhotite–arsenopyrite assemblage with Fe-bearing sphalerite. The HS deposits include enargite–luzonite–covellite paragenesis with pyrite. The IS deposits are characterized by the presence of tennantite–tetrahedrite–chalcopyrite assemblage and sphalerite with iron impurity and of rhodochrosite and anhydrite, in contrast to chalcedony and adularia of the LS deposits (Hedenquist et al., 2000). The IS deposits associated with andesite–rhyodacites formed at greater depths than the LS deposits associated with rhyolite–basalt series. The epithermal HS Au–Ag deposits are intimately associated with calc-alkalic island arc systems; their ore-forming fluids are of magmatic nature. At the near-surface level, these are cooling acid fluids that formed porphyry Cu ± Mo

✉ Corresponding author.
E-mail address: tma2105@mail.ru (A.V. Volkov)

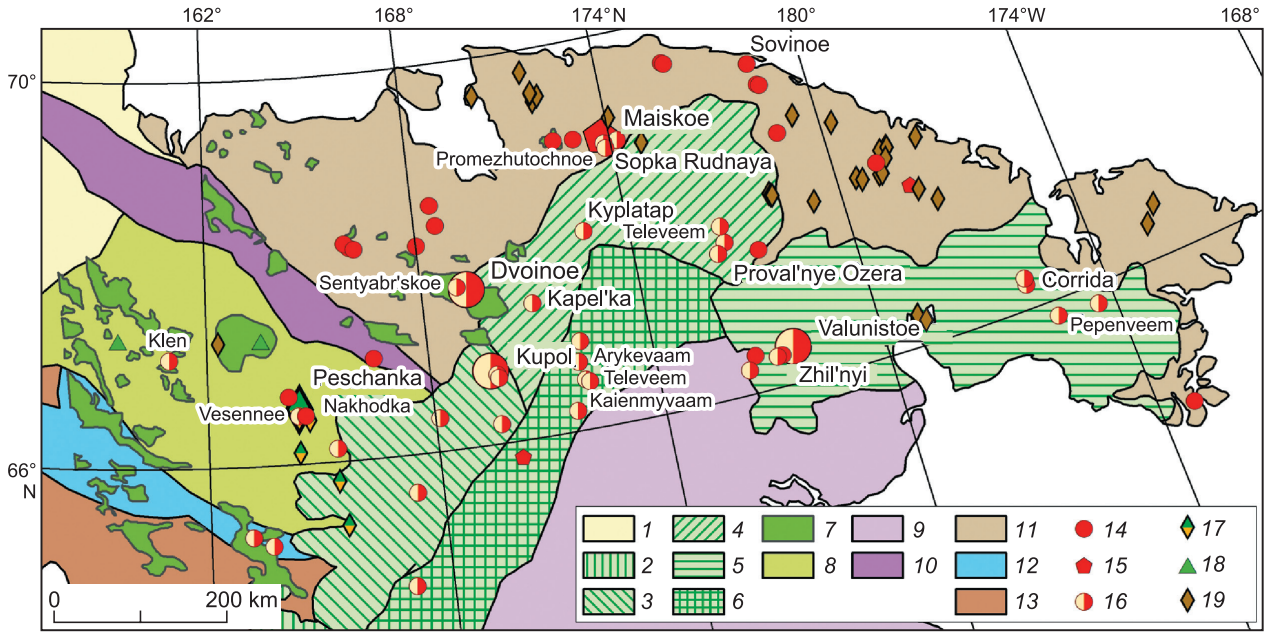

Fig. 1. Scheme of the volcanic belts and epithermal Au–Ag–Se–Te deposits of the Chukchi Peninsula, compiled after Belyi (1994), Sokolov et al. (1999), and Tikhomirov et al. (2017). *1*, Cenozoic cover; *2–6*, Okhotsk–Chukotka volcanic belt (OCVB): *2–4,* OCVB sectors: *2*, Penzhina, *3*, Anadyr', *4*, Central Chukchi; *5*, East Chukchi flank zone; *6*, inner zone of the OCVB; *7*, Early Cretaceous volcanic troughs; *8*, Oloi volcanic belt; *9*, Koryak–Kamchatka folded system; *10*, South Anyui suture; *11*, Chukchi folded system; *12*, Paleozoic–Mesozoic island arc complexes; *13*, deformed Paleozoic–Mesozoic complexes of the cover of the Omolon massif; *14–19*, ore deposits (large symbols mark large deposits, and small symbols, medium-sized and small ones): *14,* gold–quartz vein, *15*, gold–sulfide (dissemination), *16*, epithermal Au–Ag, *17*, porphyry Cu–Mo, Au- and Ag-bearing, *18*, pyrite–base-metal (in volcanic rocks), *19*, Sn ore.

± Au deposits. The almost neutral hydrothermal solutions typical of the LS deposits are usually modified meteoric waters with a minor magmatic fluid, which were heated during magmatism (Richards, 2013).

Epithermal Au–Ag deposits are associated with island arc and postaccretionary volcanic belts, slab flattening during subduction, postcollisional back-arc extension, and rift structures (Richards, 2013). These settings favored the formation of not only Au–Ag deposits but also massive sulfide (Cu–Pb–Zn–Au–Ag–Cd–In) deposits of the Kuroko and vein Kuroko types, as well as porphyry Sn–Ag, porphyry Cu–Mo–Au–Ag, and Au–As–Sb–Ag dissemination deposits (postcollisional back-arc extension).

The Chukchi Autonomous District (ChAD) is the extreme northeastern and gold-richest part of the Arctic zone of Russia (Bortnikov et al., 2015). It occupies the entire Chukchi Peninsula and a number of islands (Fig. 1). In 1955, Sidorov (1966) discovered the first epithermal Au–Ag deposits in the ChAD and in northeastern Russia. In the next 65 years, numerous epithermal Au–Ag deposits and ore occurrences were found in the district. They were confined to the Cretaceous Okhotsk–Chukotka (OCVB) continent-marginal and Late Jurassic–Early Cretaceous Oloi (OVB) island arc volcanic belts and to Early Cretaceous postcollisional volcanic troughs (Fig. 1). On the OCVB periphery, epithermal Au–Ag deposits were discovered in terrigenous flysch strata and relics of volcanic sheets (Volkov et al., 2006).

In 1999, the first gold and silver were mined from the ores of the Valunistoe epithermal Au–Ag deposit[1]. In 2008, the start of exploitation of the world's Au–Ag-richest epithermal Kupol deposit led to a "sharp rise" in gold mining in the ChAD. In 2009, the production of gold exceeded 30 tons, and the production of silver, 264 tons, which was a record for the ChAD. In 2020, 15.84 tons of gold and 106 tons of silver were mined from the deposit ores. More than 200 tons of gold and about 2000 tons of silver have been mined from epithermal ores in the ChAD since the beginning of the exploitation of Au–Ag deposits.

The main aim of this paper is to summarize the metallogenic, mineralogical, and fluid inclusion characteristics of epithermal Au–Ag mineralization, compare them with each other, consider the causes of the differences between the deposits, and refine the genetic model. Study of the composition and parameters of ore-forming fluids for elucidating their nature has been one of the acute problems in the theory of endogenous ore formation for decades (Bortnikov, 2006).

In addition to gold and silver, the ores of epithermal deposits contain by- and co-product metals of special interest. For example, Au and Ag chalcogenides are crucial concentrators of Se and Te, especially in epithermal deposits (Plotinskaya and Kovalenker, 2008). In recent years, the high-tech industry demand for Se and Te has increased (Bortnikov et al., 2016). Therefore, study of the distribution of Se and

[1] Valunistyi mine (russdragmet.ru)

Te in the ores of the epithermal deposits of the Chukchi Peninsula is of great practical importance.

The information given in this paper can be applied during regional predictive metallogenic mapping and in the search for and assessment of epithermal Au–Ag deposits.

BRIEF DESCRIPTION OF THE VOLCANIC BELTS AND EPITHERMAL Au–Ag DEPOSITS OF THE CHUKCHI PENINSULA

The epithermal Au–Ag deposits of the Chukchi Peninsula are controlled by volcanic belts of different ages superposed on terranes (Fig. 1). The accretion of the terranes terminated in post-Hauterivian/pre-Albian time and fixed the position of the newly formed continental margin, whose basement is mostly the Precambrian continental crust (Khanchuk, 2006). The accreted terranes include the Chaun and Anyui subterranes of the passive continental margin, the South Anyui terrane (a fragment of the Jurassic–Early Cretaceous subduction zone), and fragments of the Early Cretaceous island arcs and the late Paleozoic–early Mesozoic continental margin, which form a heterogeneous basement for the volcanic belts.

The OCVB is parallel to the current Kuril–Kamchatka Trench. The OVB is parallel to the Late Jurassic northern continental paleomargin (Sokolov et al., 1999) and orthogonal to the OCVB (Fig. 1). The OVB and other structures located southwest and northeast of the South Anyui suture are superposed by the Aptian continental volcanic troughs that formed after the Hauterivian–Barremian closure of the South Anyui ocean basin caused by the collision of the Chukchi microcontinent with the active margin of the Siberian continent. The closure was accompanied by the termination of suprasubductional magmatism in the Oloi belt (Tikhomirov et al., 2017; Sokolov et al., 2021). Thus, the OCVB strata overlap the rocks of the Aptian volcanic troughs and OVB within the western Chukchi Peninsula.

The **Oloi volcanic belt** is controlled by the Late Jurassic–Early Cretaceous paleoisland arc system located between the South Anyui suture and the Omolon terrane (Fig. 1). It extends for 400 km in the northwestern direction (within the Chukchi Peninsula) and is 200 km in width in the central part. The preserved OVB fragments are composed of basaltic andesites and basalt–andesite–rhyolite associations. Numerous porphyry Cu–Mo and epithermal Au–Ag deposits are associated with the magmatism of this paleoisland arc. Cu–Mo stockworks are localized in stocks and small massifs of the gabbro–monzonite–syenite series, and epithermal Au–Ag veins and deposits formed on their periphery. A characteristic feature of the OVB ore mineralization is the wide spread of magnetite (Shpikerman, 1998). This is apparently due to the substrate of the belt formed by oceanic blocks and fragments of the Precambrian Fe-quartzite-containing rocks of the Omolon block.

The Baimka metallogenic zone extends for 80 km and is 6–18 km in width in the central part of the OVB. It includes numerous Au- and Ag-containing porphyry Cu, porphyry Mo–Cu, and epithermal Au–Ag deposits and ore occurrences. The central and northern parts of the Baimka zone coincide with the southeastern block of the Kur'ya volcanic trough. In the east of the Baimka zone, within the Baimka ore district, there are Cu–Mo–Au–Ag stockworks (Peschanka and Nakhodka deposits) confined to syenite and monzonite massifs and associated with placers of high-fineness gold with rare platinum group elements (PGE).

The Vesennee Au–Ag deposit is located on the western flank of the Nakhodka porphyry Cu deposit and is confined to outcrops of the quartz monzodiorite-porphyry and porphyrytic diorites of the Yegdygkych complex (144–139 Ma, according to U–Pb dating (Nikolaev et al., 2016)) and to their proximal exocontacts composed mainly of Volgian (Upper Jurassic) sedimentary rocks (Volkov et al., 2006).

Early Cretaceous volcanic troughs. North of the South Anyui suture, there is the Tytyl'veem postcollisional trough of Aptian age (according to zircon dating) (Tikhomirov et al., 2017), 110 × 35 km in plan, extending in the northwestern direction conformably with the strike of major folded Mesozoides (Fig. 1). The relics of volcanic fields, localized in the same structures as the Tytyl'veem trough rocks, are traced for more than 300 km to the northwest along the South Anyui suture. The basement of the Tytyl'veem trough is formed by Berriasian–Hauterivian sandstones and siltstones with lenses of limestones and conglomerates (Tikhomirov et al., 2017).

The large Dvoinoe Au–Ag deposit is confined to the eastern part of the Ilirnei paleocaldera complicating the Tytyl'veem trough at the boundary with the Tytyl'veem granitoid massif (Fig. 1). The caldera is oval (14 × 6 km) and is bounded by conjugate arcuate faults steeply dipping (75–80º) toward the center of the structure. The host rocks are andesites and andesitic tuffs of Aptian age (120–118 ± 1 Ma, $^{40}Ar/^{39}Ar$ dating) (Akinin et al., 2015; Sakhno et al., 2019; Thomson et al., 2021). In the west of the Ilirnei paleocaldera, within the volcanic dome, there is the Sentyabr'skoe deposit. Most of its Au–Te mineralization is localized in a pipe-like body of explosive breccias (with fragments of andesites, basaltic andesites, and quartz), about 120 m in diameter (Fig. 2) (Savva et al., 2016; Thomson et al., 2021).

On the northwestern flank of the OVB, in the Krichal volcanic trough, the Klen Au–Ag deposit has been best studied (Fig. 1, Table 1), and several promising ore occurrences (Yunost', Ikar, Vyaz, and Iva) have been identified (Nikolaev et al., 2020). The Klen deposit is localized in the volcanic strata of the Early Cretaceous Elgechan basalt–andesite–dacite–rhyolite complex, which are intruded by subvolcanic bodies and dikes of the same age and composition.

The OCVB, an Au–Ag-bearing belt of world importance, is not inferior to the Andean and Balkan–Carpathian metallogenic belts, except for its exploration. According to Akinin (2012), the OCVB magmatism was developed from

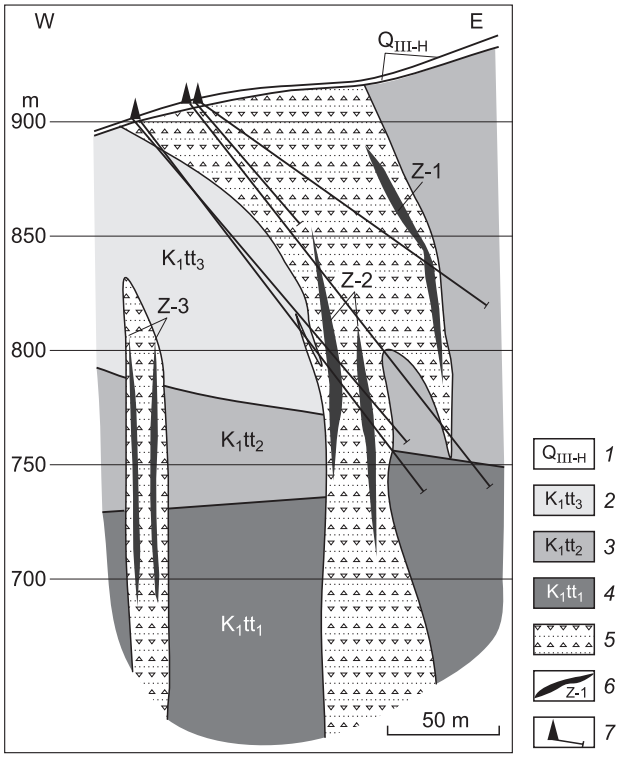

Fig. 2. Section of the ore-hosting pipe-like breccia body at the Sentyabr'skoe deposit. *1*, deluvial sediments: gravel, sands, and clays; *2–4*, Tytyl'veem Formation: *2*, andesites and their tuffs and clastolavas (K_1tt_3), *3*, rhyolites, rhyodacites, dacites, andesites, their tuffs, ignimbrites, tuff conglomerates, tuffstones, and tuff argillites ($K1tt_2$), *4*, andesites, basaltic andesites, trachyandesites, their clastolavas and tuffs, tuffstones, tuff argillites, and, seldom, tuff conglomerates (K_1tt_1); *5*, explosive breccias; *6*, enriched sites (ore zones) of the ore-hosting breccia; *7*, core boreholes.

middle Albian to middle Campanian (106–78 Ma), which correlates with the change in the rate of the motion of the Paleopacific Izanagi and Kula oceanic plates. Most of volcanic material was erupted in the Coniacian and Santonian.

The Chukchi segment of the belt is about 1500 km long and 100–300 km wide. The OCVB is composed solely of subaerial calc-alkalic and, partly, subalkalic volcanic rocks (alumina basalts–andesites–dacites–rhyolites) up to 5–7 km in thickness as well as compositionally similar and nearly coeval intrusions, often batholith-like, mostly multiphase, composed of gabbro, diorites, predominant granodiorites (including tonalites and quartz monzonites), and granites. The geologic structure and metallogeny of the OCVB are widely covered in literature (Umitbaev, 1986; Belyi, 1994; Sidorov et al., 2009) and, therefore, are not considered in detail here.

The main structures of the Chukchi part of the OCVB are shown, after Belyi (1994), in Fig. 1. The East Chukchi flank zone of the OCVB overlaps mainly the structures of the pre-Riphean Eskimo median mass. The inner zone of the OCVB is superposed on the Amguem flysch and Erguveem ophiolite subterranes and on the Kanchalan shelf subterrane with a metamorphic basement of tentatively Proterozoic age.

The outer zone of the OCVB is divided into two sectors within the Chukchi segment: Anadyr' and Central Chukchi, which differ in magmatism evolution, volumes of volcanic strata, and structure.

In the Anadyr' sector, the basement of volcanic sheets in the outer zone is formed by the OVB and Berezovka terrane structures, and in the Central Chukchi sector, by the structures of the Chukchi fold belt.

In the Central Chukchi sector, there is a sharp bend of the boundary between the outer and inner zones of the OCVB, and the strike of the belt changes from northeastern to southeastern (Fig. 1). In contrast to the rest regions, the evolution of the Central Chukchi sector began with the formation of ignimbrite strata and, then, andesite nappes. At the Chukchi segment of the OCVB, there are numerous epithermal Au–Ag deposits; the main ones are shown in Fig. 1.

Ore-bearing structures of the OCVB. Volcanotectonic depressions (VTD) and ancient calderas are the most crucial structures controlling the localization of epithermal Au–Ag deposits in the OCVB areas of contrasting volcanism. These are the structures where the intimate paragenetic and genetic relationship among tectonics, volcanoplutonic complexes, metasomatism, and ore mineralization is best manifested. At the same time, in the OCVB areas of basaltic volcanism, the localization of ores is greatly controlled by positive volcano dome structures resulted from the intrusion of subalkalic granitoids. The epithermal Au–Ag deposits and ore occurrences are confined to the margins of volcanotectonic troughs and to the periphery of rigid structures in the belt basement (Sidorov et al., 2009).

The Au–Ag mineralization of the Chukchi segment of the OCVB is characterized by the greatest diversity of minerals, which is determined both by their localization relative to the metallogenic zones adjacent to the OCVB and by the degree of differentiation of the Au–Ag systems. The characteristics of the main Chukchi epithermal Au–Ag deposits are presented in Table 1.

The Kupol deposit (Sidorov et al., 2008), the largest one in the OCVB, can be regarded as "unusual". In the area of his deposit, the essentially basalt–andesite section of the Anadyr' sector of the belt (homodrome sequence) changes to the essentially rhyolite–dacite–basaltic-andesite section of the Central Chukchi sector (antidrome sequence) within a short distance (Belyi et al., 2008). The deposit is confined to the center of a caldera 10 km in diameter located on the northwestern margin of the Upper Cretaceous Mechkereva VTD about 100 km in width (Vartanyan et al., 2005). Paleoreconstruction showed that the Kupol deposit was, most likely, localized in the northwestern sector of a shield-like andesitic paleovolcano, which appeared after the formation of the paleocaldera and was discovered in the OCVB for the first time (Belyi et al., 2008).

In the central part of the paleovolcano, near the eruption site, there are Au–Ag sulfosalt deposits (Kupol, Moroshka, and Prikup), and on the periphery, on the slopes of the stra-

Table 1. Characteristics of the main epithermal Au–Ag–Se–Te deposits and promising ore occurrences of the Chukchi Peninsula

Deposit	Position in regional volcanic structures	Igneous rocks	Host rocks, association	Resources, tons		Content, ppm		Ag/Au	Subtype	Se and/or Te minerals
				Au	Ag	Au	Ag			
East Chukchi flank zone of the OCVB										
Valunistoe	Il'enei–Amguem semigraben, East Chukchi zone of the OCVB	Volcanic-dome structure, basaltic-andesite and basalt dikes	Ignimbrites, lavas, tuffs, and tuff breccias of rhyolitic to basaltic composition	17.5 (40)	178 (279)	5.9 (10.7)	59.6 (74.7)	10 (7)	Se, Te	Naumannite, Se-acanthite, hessite, matildite
Zhil'noe	Il'enei–Amguem semigraben, East Chukchi zone of the OCVB	Volcanic-dome structure, basaltic-andesite and basalt dikes	Ignimbrites, lavas, tuffs, and tuff breccias of rhyolitic to basaltic composition	(10)	(1272)	13.8	1696	12.7	Se, Te	Naumannite, Se-acanthite, hessite
Corrida	Pikhcha VTD, East Chukchi zone of the OCVB	Volcanic-dome structure, rhyolite and basaltic-andesite dikes	Crystalloclastic rhyolitic and rhyodacitic tuffs	(37)	(340)	15	135	9	Se	Naumannite, clausthalite, Se-acanthite, fischesserite
Pepenveem	Erguveem VTD, East Chukchi zone of the OCVB	Pepen intrusive-dome uplift, necks of rhyolites and their lava breccias	Andesites, tuffs, and rhyodacitic ignimbrites	(61)	(2860)	5.3	250	47	Se	Se-acanthite, naumannite
Inner zone of the OCVB										
Arykevaam	Kaienmyvaam uplift, inner zone of the OCVB	Cryptointrusive dome, subvolcanic andesite and diorite bodies	Ignimbrites, rhyolites, andesites, and their tuffs	3.8	273	4.5	324	71	Te	Hessite, petzite, tellurobismuthite, volynskite, kawazulite
Televeem	Kaienmyvaam uplift, inner zone of the OCVB	Caldera complex, subvolcanic andesite and diorite bodies	Andesites and their tuffs	(37)	(62.9)	30	51.8	1.7	Te	Sylvanite, petzite, tellurobismuthite, altaite, hessite, volynskite
Kaienmyvaam	Kaienmyvaam uplift, inner zone of the OCVB	Caldera complex, subvolcanic rhyolite and basaltic-andesite bodies	Ignimbrites, rhyolites, andesites, and their tuffs	(9.6)	(76.5)	26.8	214.4	8	Te	Petzite, hessite, alltaite, sylvanite, tellurobismuthite
Central Chukchi sector of the OCVB										
Promezhutochnoe (northeast)	Western flank of the Pegtymel' volcanic trough, Central Chukchi sector of the OCVB	Intrusive-dome structure, basaltic-andesite dikes	Siltstones with sandstone lenses	1.5 (5)	15 (50)	12	120	10	Se	Naumannite, Se-acanthite, Se-miargyrite, Se-pyrargyrite
Kupol	Kaemraveem VTD, Anadyr' sector of the OCVB	Shield paleovolcano, subvolcanic rhyolite and basaltic-andesite bodies	Two-pyroxene plateau andesites, basaltic andesites, and their tuffs	180	2160	21,5	258	12	Se	Fischesserite, Se-acanthite, naumannite, Se-stephanite, Se- pyrargyrite
Kapel'ka	Ugatka VTD, Central Chukchi sector of the OCVB	Volcanic-dome structure, subvolcanic andesite, rhyolite, and diorite bodies	Andesite–dacite–rhyodacite association	(26.1)	(1600)	12.8	916	61	Se	Se-polybasite-pearceite, Se-tennantite
Sopka Rudnaya	Western flank of the Pegtymel' volcanic trough, Central Chukchi sector of the OCVB	Caldera complex, subvolcanic basaltic-andesite bodies and dikes	Andesite–dacite–rhyolite association, siltstones with sandstone lenses	2.0 (4)	25 (50)	16.3	203	12.5	Se	Fischesserite, Se-stephanite, Se-argyrodite, naumannite
Oloi volcanic belt										
Vesennee	Baimka zone of the OVB	Nakhodka volcanic structure, Egdygkych gabbro–monzonite–syenite complex	Tuff conglomerates, tuffstones, basaltic andesites, andesites, tuffs, and eruptive breccias	14.8 (359)	75.2 (3099)	3.6 (1.5)	18.4 (13)	5 (8.6)	Te	Hessite, cervelleite, petzite
Early Cretaceous volcanic troughs										
Dvoinoe	Tytyl'veem	Illirnei caldera complex, subvolcanic rhyolite bodies	Andesites and their tuffs	64	94	18.6	27.0	1.5	Se, Te	Hessite, goldfieldite
Sentyabr'skoe	Tytyl'veem	Volcanic dome, subvolcanic bodies of quartz monzonites and rhyolites	Andesites, basaltic andesites, rhyolite tuffs, and lava breccias	2.2	1.1	60	30	2	Te	Petzite, hessite, altaite, coloradoite
Klen	Krichal'	Krichal' volcanic graben	Basalt–andesite–dacite–rhyolite association	18.7 (60)	43.8 (140)	9.4	21.6	2.3	Se, Te	Se-polybasite, naumannite, hessite

Note. OCVB, Okhotsk–Chukotka volcanic belt; OVB, Oloi volcanic belt; VTD, volcanotectonic depression.

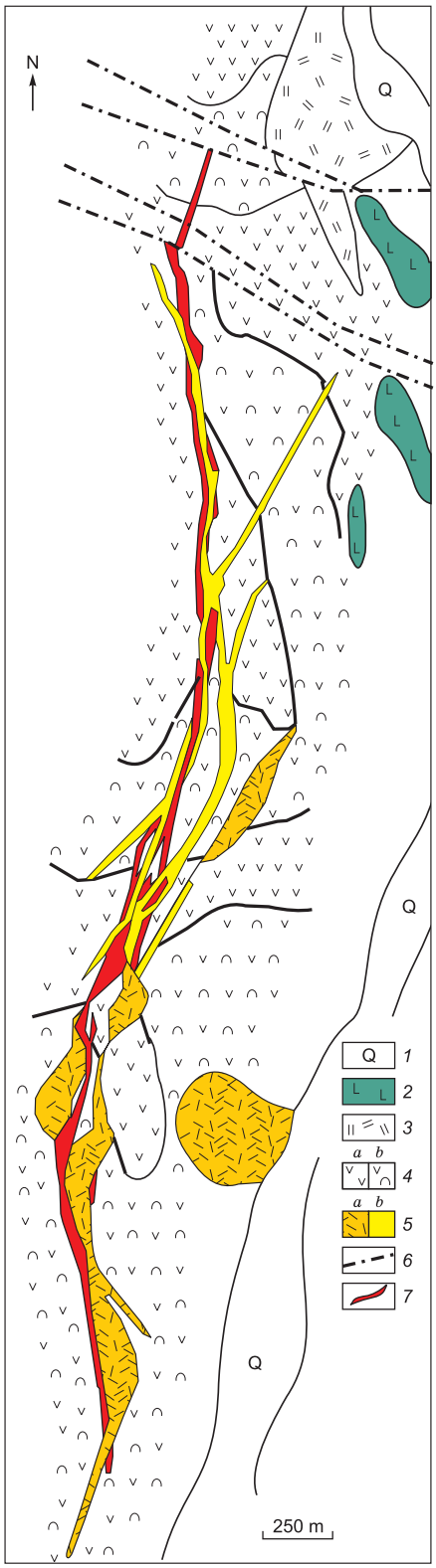

Fig. 3. Schematic map of the Kupol deposit. *1*, Quaternary alluvial deposits, *2*, Paleogene basalt nappes; *3*, *4*, Late Cretaceous volcanic rocks: *3*, upper strata: rhyolites, *4,* middle strata: interbedding of andesites and basaltic andesites (*a*) and agglomerate lapilli and ash tuffs (*b*); *5*, Late Cretaceous rhyolites of the dome complex (*a*) and rhyolite and rhyodacite dikes (*b*); *6*, faults; *7*, orebodies: adularia–quartz veins and veinlet zones.

tovolcano, galena–sphalerite Au–Ag mineralization is found (Dublon and Tokai ore occurrences) (Lorentz and Sergievski, 2009). The U–Pb (SHRIMP) age of the host volcanic rocks is 94.8 ± 1.4 Ma, and the age of the upper nappe andesites is 89.5 ± 2 Ma (Sakhno et al., 2019). The total thickness of the volcanic sequence is 1300 m.

The main orebody of the Kupol deposit (OB 1) is more than 3000 m in length and 1 to 21 m in thickness. It was traced by core drilling to a depth of 530 m, which is not typical of epithermal Au–Ag deposits (Volkov et al., 2012). The orebody is cut by large rhyolite dikes almost throughout its length (Fig. 3). It is of N–S strike and is formed by subparallel en-echelon proximal quartz veins dipping to the east at 75–85º and, more seldom, by breccias with quartz cement. The wallrock metasomatic alterations are highly diverse: from low-temperature argillization to high-temperature biotitization. There are also alunite–jarosite metasomatites resulted from the paleosolfatara activity. They are developed after the groundmass of volcanic rocks to a depth greater than 400 m (Savva et al., 2012) and were earlier taken for oxidized ores (Vartanyan et al., 2005). The latest SHRIMP data suggest the formation of the Kupol deposit in the interval 89–88 Ma (Sakhno et al., 2019).

In the outer zone of the Central Chukchi sector of the OCVB, the Pegtymel' compensation volcanic trough extending in the northeastern direction (Fig. 1) is the largest structure. In the southeast, the trough is open toward the inner zone and adjoins the southeastern segment of the boundary between the outer and inner zones of the OCVB. On the periphery and inside the Pegtymel' trough, there are widespread porphyry Cu–Mo, Sn–Ag, Au–sulfide dissemination, Au–Bi, Au–Ag, Sb–Hg, and Hg deposits. The Sopka Rudnaya and Promezhutochnoe Au–Ag deposits and the Kyplatap ore occurrence are localized on the northwestern flank of the trough, and the Televeem and Proval'nye Ozera ore occurrences, on the eastern flank (Fig. 1).

The Sopka Rudnaya deposit is localized in an eroded remnant of effusive nappe rocks in the outer zone of the Pegtymel' volcanic trough in the southeastern sector of the Kukenei intrusive-dome structure. The Promezhutochnoe deposit is confined to the dome at the southern closure of this structure. The volcanic rocks of the ore field are completely eroded. The distance from them to the effusive nappe of the OCVB is no more than 15 km.

The Uteveem ore cluster, including the Kapel'ka Au–Ag ore occurrence, is located in the central part of the large Pucheveem VTD in the Central Chukchi sector of the OCVB (Fig. 1). The age of the host volcanic rocks is 87 Ma (Tikhomirov et al., 2012). Mineralization occurs in vein zones about 1.5 km in length and 50–350 m in width and in isometric stockwork-like veinlet systems. The main wallrock alterations are propylitization, argillization, and transformation into quartzites.

In the inner zone of the OCVB, all known Au–Ag deposits (Irgunei, Kaienmyvaam, Televeem, Kvartsevyi, Arykevaam, and Enmyvaam (listed in the order of location from

southwest to northeast)) are within the graben trough area (Fig. 1).

The deposits of the best studied ***Kaienmyvaam ore district*** are located on the southern and northern slopes (flanks) of a relict volcanic uplift between troughs (Volkov et al., 2020). In the present-day erosional truncation, the core of the uplift, up to 10 km across, is composed of the massive porphyroclastic rhyolite ignimbrites of the Pykarvaam Formation. It is framed by the rocks of the Koekvun' (andesites) and Ergyvaam (rhyolites) formations. There are also widespread argillizite–secondary quartzite caps within the uplift (Belousov et al., 2020). The Arykevaam deposit is localized in the dome structure at the northern closure of the uplift, and the Kaienmyvaam and Televeem ore occurrences are confined to proximal negative volcanotectonic structures in the central and southern parts of the uplift. The likely orebodies are veins up to 20 m thick (in swells) and up to 300 m long, with colloform–banded, framework–lamellar, breccia, banded, and massive structures. Epithermal HS Au–Ag deposits are predicted within the inner zone of the OCVB (Prokofiev, 2019b).

The East Chukchi flank zone is divided into three large volcanic areas: Erguveem, Kanchalan, and Vul'vyveem. The former two contain Au–Ag deposits.

The Erguveem area is isometric, 80–90 km in diameter, and composed of andesites, rhyodacites, basalts, and trachybasalts. Its basement is formed by the island arc rocks of the Vel'mai terrane (Ledneva et al., 2016). Andesites (Buor-Kemyus Horizon, Nyrvakinot Formation, 500–600 m) and dacite–rhyolite associations (Arman Horizon, Amgen Formation, 600–700 m) are predominant. Younger rocks compose certain volcanic structures or their fragments.

The Corrida deposit is localized in the field of the rhyolites and rhyodacites of the Amgen' Formation and is controlled by the Pichkhin VTD, and the Pepenveem ore field is confined to the remanent volcanic-dome uplift composed of the andesites of the Nyrvakinot Formation. Argillizites and secondary quartzites are widespread in the ore fields (Volkov et al., 2006).

In *the Kanchalan area*, rocks of basaltic-andesite–rhyolite association are widespread. In the Il'enei–Amguem semigraben (more than 200 km long and 20–50 km wide) in the north of the area, volcanic-dome structures 3–6 km in diameter are major ore-controlling objects. They form a NE striking chain along the graben and host several epithermal Au–Ag deposits (Valunistoe, Gornoe, and Zhil'noe) and promising ore occurrences (Ognennoe, Shakh, Oranzhevoe, etc.).

ORE STRUCTURES

The mineral structures of most of the Au–Ag ores of the Chukchi deposits are typical of epithermal deposits, with rhythmic and colloform–banded pattern units with significant amounts of chalcedony-like and crustified quartz. The ores are predominantly finely disseminated, often with bands of ore minerals (ginguro) (Fig. 4). The vein cores sometimes have a framework–lamellar structure. The vein structures are diverse; these are generally "filling" structures. The crustification and cockade structures of the vein bodies are evident of pulsed ore formation.

The breccia texture is characterized by the replacement of fragments of the host rocks by quartz (Fig. 4*e*). After silicification, only fragment relics are preserved. They are called "shadows", and such breccias are called "shadow" breccias. The breccia texture is typical of the vein selvages containing elongate plates of the altered host rocks (Fig. 4*c*, *j*, *m*).

The ore-bearing veins of most deposits are characterized by complex breccia–crustification textures. Such vein bodies are "composite", with the volume ratio of quartz and host-rock relics varying from 1:10 to 10:1 and in wider ranges. The composition of the rock fragments often differs from that of the enclosing rocks, because they might have been transferred for significant distances. The fragments are differently oriented; the neighboring ones are of different shapes. All of them are present in homogeneous quartz as "matrix-supported" fragments (Fig. 4*o*, *p*).

The orebodies of the Kupol deposit are characterized by numerous breccias and megabreccias with cockade overgrowth of fragments of different compositions with quartz and amethyst (Fig. 4*n*). The productive veins of the Dvoinoe deposit (Fig. 4*m*) have breccias with fragments of quartz of early generations, which are cemented by late metacolloidal quartz. In addition, there are postore breccias with fragments of the host rocks and quartz veins cemented with carbonate, as in the Valunistoe deposit (Volkov et al., 2020). The ores of the Sentyabr'skoe deposit are predominantly of breccia and veinlet structures, and colloform–banded structures are observed in the deconsolidated parts of breccias (Fig. 4*g*, *k*). The orebodies of the Promezhutochnoe deposit localized in siltstones are characterized by transitions from breccia to framework–lamellar and crustification structures (Fig. 4*c*), which makes them strongly different from gold–quartz veins (Firsov, 1980) also localized in terrigenous strata. The deposit vein fragments with framework–lamellar and crustification structures have cavities, often filled with large quartz druses (the quartz crystals sometimes reach 3–5 cm in size (Fig. 4*j*)) or unique quartz roses and branched coral-like quartz–antimonite aggregates (Volkov and Prokof'ev, 2011).

The diversity of the structures of gold-bearing veins indicates the dynamic and rapidly changing conditions of ore formation. The colloform structures point to the mineral formation from supersaturated fluids. The crustification structures are evident of the deposition of mineral aggregates in open cavities. The breccia structures indicate a repeated inflow of fluids into the ore-forming system and a high fluid pressure exceeding the lithostatic one. These factors led to the crushing of early mineral aggregates in the cracks and their breakthrough and cementation by later ones. The above dynamic processes might have been caused by the boiling-

Fig. 4. Structures of the ores of the Chukchi epithermal Au–Ag deposits: *a–h*, colloform–banded and framework–lamellar structures: *a*, Valunistoe, *b*, Kupol, *c*, Promezhutochnoe, *d*, Corrida, *e*, Televeem, *f*, Vesennee, *g*, Sentyabr'skoe, *h*, Dvoinoe; *i–l*, druse and crustification structures: *i*, Kupol, *j*, Promezhutochnoe, *k*, Sentyabr'skoe, *l*, Kyplatap; *m–p*, veinlet and breccia structures: *m*, Dvoinoe, *n*, Kupol, *o*, Proval'nye Ozera, *p*, Vesennee.

up of the mineral-forming fluid, which led to the separation of the low-density phase and a pressure increase.

MAJOR ORE MINERALS

The mineral composition of ores was studied in polished sections under an AXIOPLAN Imaging microscope. The chemical composition of the minerals was determined using different electron microprobes: JEOL JXA-8100 (Mineral Analysis Laboratory of the Institute of Geology of Ore Deposits, Petrography, Mineralogy and Geochemistry, Moscow, analyst I.G. Griboedova), Camebax (analysts E.M. Goryacheva and T.V. Subbotnikova), EVO50 QemScan, with a Quantax Esprit X-ray energy-dispersive microanalysis system (Northeastern Interdisciplinary Research Institute, Magadan, analyst O.T. Sotskaya), and JEOL JSM-6510LVSEM (Institute of Geology and Mineralogy, Novosibirsk, analyst N.S. Karmanov). The fineness of native gold was calculated with the GOLD software (designed by S.V. Preis). Below we report in brief the results of mineralogical studies of the Chukchi epithermal Au–Ag deposits.

Native gold of these deposits is commonly of low fineness, with medium to high dispersion of its value (Fig. 5), which is also typical of deposits of this genetic class in other regions of the world (Simmons et al., 2005). Intrusive magmatism led to the metamorphism of ores, increasing the degree of their differentiation (Kupol, Televeem, Corrida, and Promezhutochnoe deposits); this influenced the distribution of gold fineness (Fig. 5).

Native gold is characterized by different aggregation states. It is found mostly as xenomorphic or interstitial (in quartz) segregations (Fig. 6). Most often, it is deposited in the interstices of vein minerals (Fig. 6*e*); sometimes, it occurs as single grains, predominantly rhombododecahedral.

The steeply gradient conditions of formation of the epithermal Au–Ag deposits determined predominantly fine-grained ore mineralization and, particularly, native gold (Fig. 6*e*). There are also intergrowths of native gold with sphalerite, galena, chalcopyrite, acanthite, silver sulfosalts,

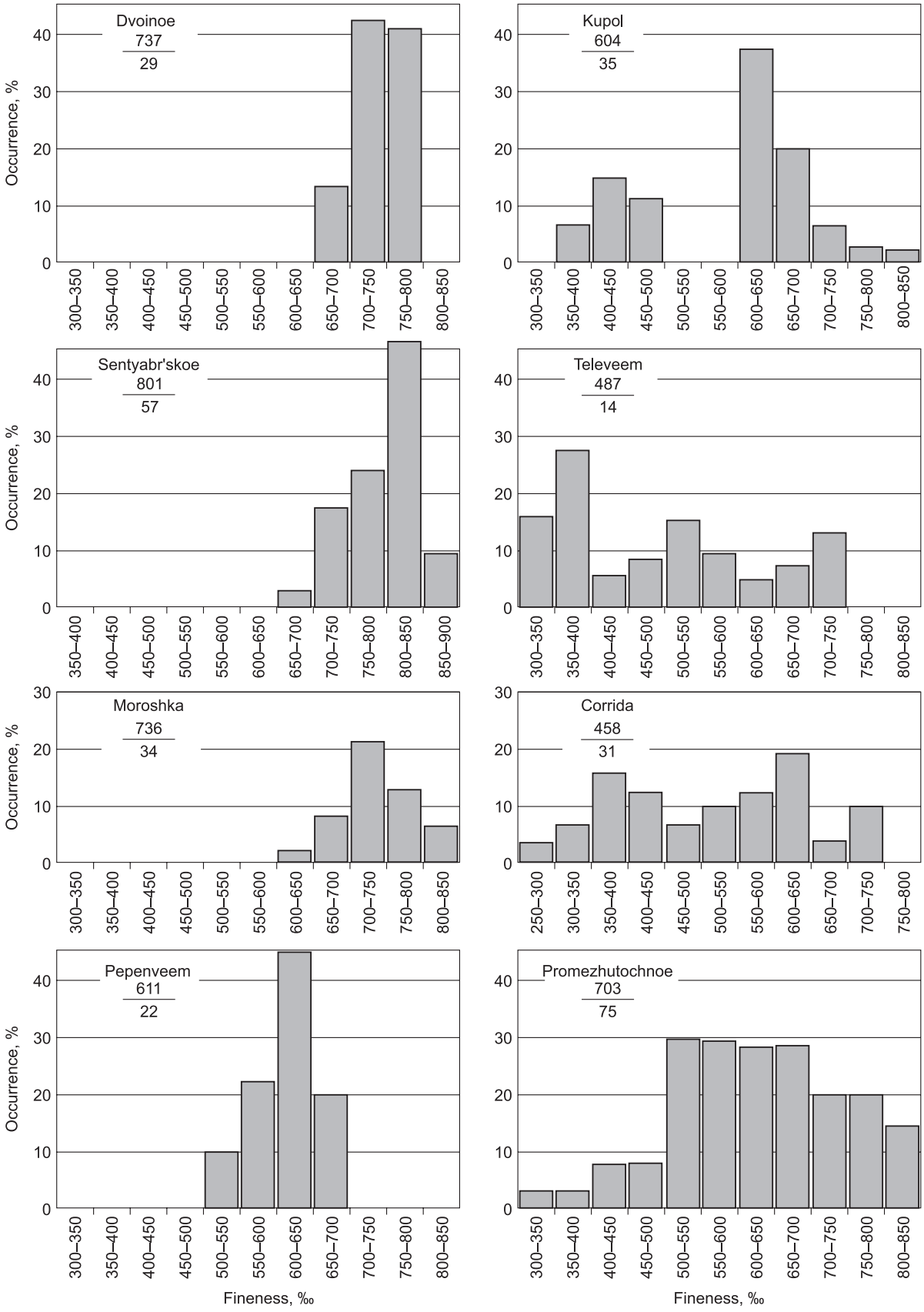

Fig. 5. Histograms of the fineness of native gold at the Chukchi epithermal Au–Ag deposits. The number above the line marks the average fineness, ‰, and that below the line is the number of measurements.

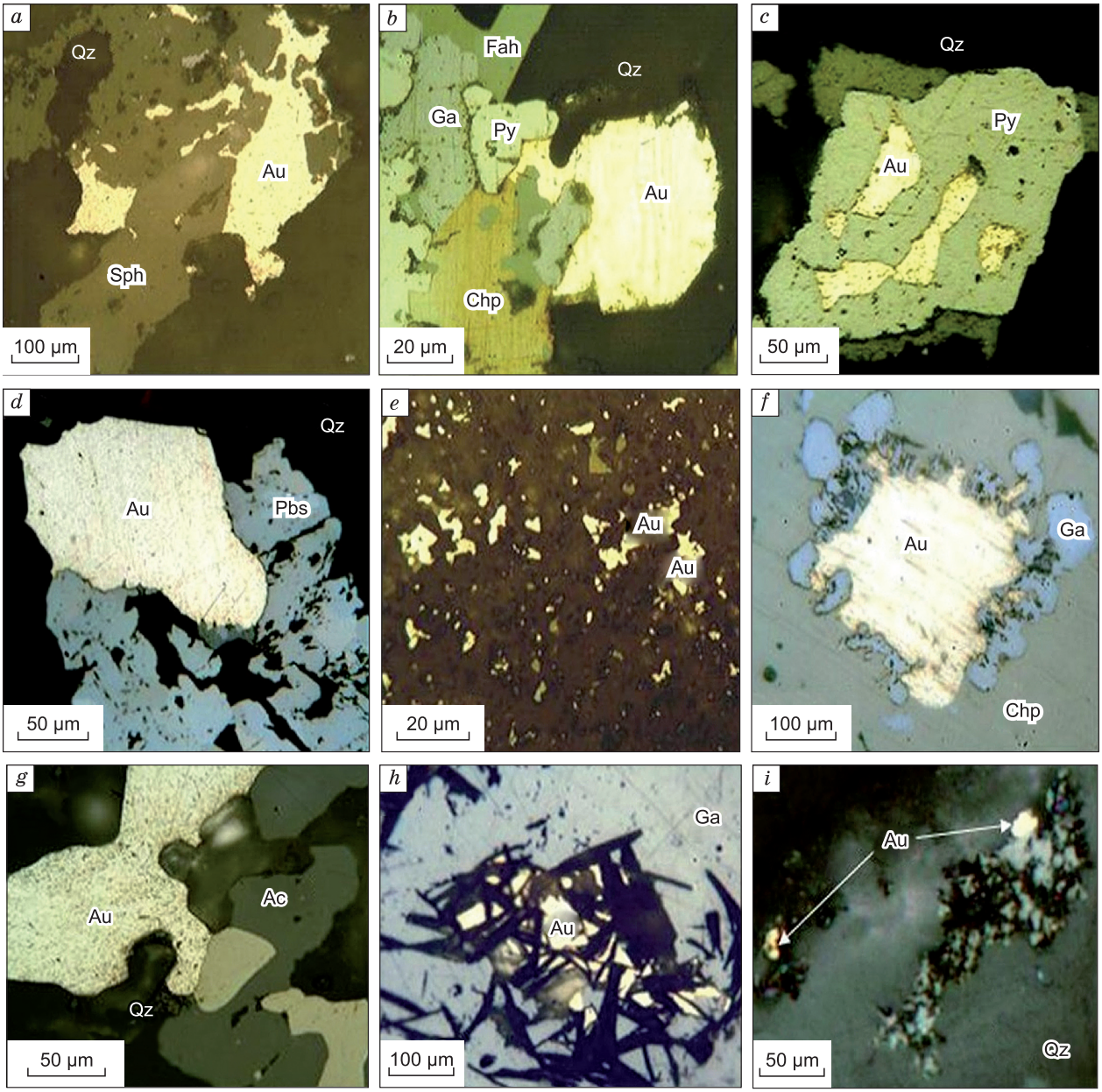

Fig. 6. Mineral intergrowths and segregations of native gold in the ores of the Chukchi epithermal Au–Ag deposits. *a*, Gold intergrown with sphalerite (Kupol); *b*, gold intergrown with pyrite, chalcopyrite, galena, and fahlore (Dvoinoe); *c*, gold inclusion in pyrite (Kupol); *d*, gold intergrown with polybasite (Kupol); *e*, fine native gold in quartz (Dvoinoe); *f*, native-gold segregation in chalcopyrite, framed by galena from explosive breccia (Sentyabr'skoe); *g*, gold intergrown with acanthite (Kaienmyveem); *h*, gold intergrown with muscovite in galena (Sentyabr'skoe); *i*, gold intergrown with flocculent acanthite (Kyplatap). Ac, acanthite, Chp, chalcopyrite, Ga, galena, Fah, fahlore, Pbs, polybasite, Py, pyrite, Sph, sphalerite, Qz, quartz.

fahlore, muscovite (Fig. 6*a–d*, *h*, *i*), and less widespread hessite.

At the Sentyabr'skoe deposit, Au–Ag mineralization is related to explosion. There are widespread spheroids with superposed segregations of native gold and galena (Fig. 6*f*). Below, we present examples of various native-gold intergrowths (Fig. 6).

Acanthite is a widespread mineral in the ores of the epithermal Chukchi deposits. Its highest contents are typical of deposits with multiple redistribution of substance (Kupol, Corrida, Televeem, and Valunistoe). These deposits are usually regarded as acanthite or Ag-acanthite ones. The mineral is well preserved under hypergene conditions and accumulates in supraore zones, forming local anomalies of Ag (with its contents exceeding those in ores), which can be used as a search criterion.

Acanthite is intergrown with various minerals (galena, sphalerite, chalcopyrite, fahlores, and native gold), but we

present its most common intergrowths (Fig. 7), namely, rims on galena and a rhythmically banded aggregate developed after Ag-containing minerals in oxidation zone. The grains are predominantly xenomorphic. Acanthite is also intergrown with aguilarite and naumannite. It contains impurities of Cu, As, Se, and, more seldom, Fe, which reflect the geochemical specifics of the ore formation environment. This mineral is characterized by both cationic and anionic isomorphism. Acanthite solid solution has a variable composition Ag_2S–$Ag_2S_{0.4}Se_{0.6}$, which determines wide variations in

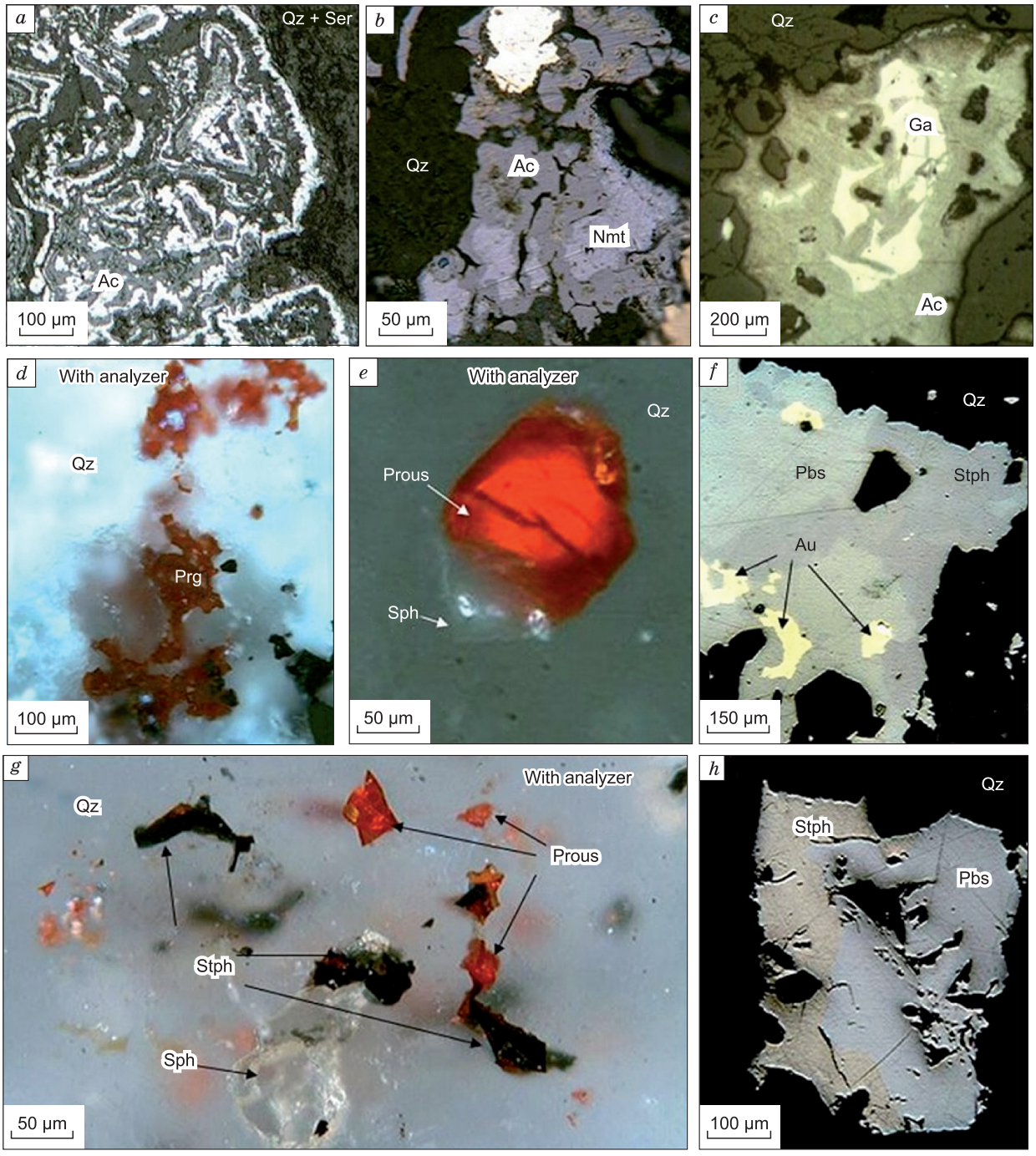

Fig. 7. Acanthite and Ag sulfosalts in the ores of the Chukchi epithermal Au–Ag deposits. *a,* Colloform segregation of acanthite in quartz–sericite matrix (Kyplatap); *b*, acanthite intergrown with naumannite and with native-gold inclusion (Kaienmyvaam); *c*, acanthite deposition around galena (Corrida); *d*, xenomorphic segregations of pyrargyrite in quartz (Kupol); *e*, euhedral segregation of proustite intergrown with colorless sphalerite in quartz (Moroshka); *f*, disordered intergrowth of polybasite with stephanite, with native-gold segregations (Televeem); *g*, interstitial segregations of stephanite and proustite in quartz and transparent sphalerite crystal (Moroshka); *h*, intergrowth of polybasite and stephanite in quartz (Pepenveem); *e*, *g*, with analyzer. Ac, acanthite, Ga, galena, Nmt, naumannite, Prg, pyrargyrite; Prous, proustite, Pbs, polybasite, Ser, sericite, Sph, sphalerite, Stph, stephanite, Qz, quartz.

Se content in the mineral (Pingitore et al., 1992, 1993; Bindi and Pingitore, 2013; Zhuravkova et al., 2015, 2019). In long-developed systems (multistage and multiphase) with thermal metamorphism, late generations of acanthite are refined from impurities.

Naumannite is a selenium mineral found in the ores of almost all Chukchi deposits; sometimes it is present in significant amounts (Corrida, Kaienmyvaam, Kupol, and Promezhutochnoe deposits). In places, selenium is removed from coalified sedimentary strata and intermediate reservoirs and is deposited in the ores of epithermal Au–Ag deposits (during their breakthrough by volcanic structures). Naumannite is often intergrown with acanthite (Fig. 7*b*).

Corrida is a typical gold–silver–selenide deposit. The chalcedony of this deposit contains finely disseminated ore mineralization with a large amount of silver selenides, associated with Ag–Cl–Br minerals (chlorargyrite and bromargyrite). This phenomenon might be due to seawaters buried in the base of the volcanic edifice (Kolova et al., 2021).

Uytenbogaardtite is often found in the ores of the Chukchi epithermal deposits. Usually it forms rims on native gold, xenomorphic clusters, and ≥10–20 μm wide veinlets; sometimes it occurs as solid mass, earthy aggregates, isolated microinclusions in native gold, and, more seldom, monolithic grains up to 3–4 mm in size. In addition to uytenbogaardtite, more rare *fischesserite* and *penzhinite* were found.

Silver sulfosalts (miargyrite, pyrargyrite, proustite, polybasite, and pierceite) are widespread in the ores of the Chukchi deposits. Minerals of the polybasite–pierceite group are members of two continuous solid-solution series from arsenpolybasite and polybasite $(Ag,Cu)_{16}(As,Sb)_2S_{11}$ to stibiopierceite $(Ag,Cu)_{16}(Sb,As)_2S_{11}$. At the epithermal deposits, such multicomponent minerals usually have a nonstoichiometric composition. In the ores, they are associated with galena, chalcopyrite, stephanite, fahlores, and native gold.

Stephanite, along with polybasite, is more often found in the ores of multistage deposits (Kupol, Valunistoe, and Televeem). The minerals are deposited in quartz interstices. Their grains are 0.3–0.5 mm in size, reaching 1–3 mm in some deposits (Televeem). Stephanite is intimately intergrown with polybasite in an interstice. The ores of single- and two-stage deposits (Pepenveem, Kaienmyvaam, and Valunistoe) contain silver sulfosalts with lower Ag contents, such as proustite, pyrargyrite, pirceite, and miargyrite (Moroshka and Dvoinoe deposits). Mineral intergrowths of silver sulfosalts are shown in Fig. 7.

Silver sulfosalts contain Se and Cu traces microimpurities, omitted from the accepted mineral formulae. These impurities reflect the specific metallogeny of the basement of the volcanic edifice, often indicating a small erosional truncation (Se) and a relationship of the deposit with a porphyry Cu system (Cu) (Savva, 2018).

Gold, silver, and lead tellurides were found in significant amounts in the Sentyabr'skoe and Televeem deposits (Fig. 8) (Nikolaev et al., 2013; Savva et al., 2016; Vlasov et al., 2016). In addition, hessite is seldom found in the ores of the Dvoinoe and Vesennee deposits (Table 1; Fig. 8*i*) (Volkov et al., 2018; Nikolaev et al., 2020).

At **the Televeem deposit**, tellurium minerals (sylvanite, petzite, altaite, hessite, melonite, volynskite, tellurobismuthite, and native tellurium) in the ores are in intimate association with earlier sulfides (Vlasov et al., 2016), forming drop-like or slightly elongate ingrowths up to 100 μm in size (Fig. 8*a*). Seldom, tellurides form individual xenomorphic grains 0.05 to 0.50 mm in size in vein quartz (Fig. 8*b*, *c*). Single inclusions of native tellurium were found in chalcopyrite and tetrahedrite-(Zn). The most numerous segregations of tellurides are observed in bornite. The lattice bornite "exsolution-like" texture is cut by telluride aggregates, which confirms the later deposition of the latter (Fig. 8*a*). Sylvanite and petzite are the main gold minerals in this paragenesis. They compose both monomineral drop-like inclusions in the bornite and irregular-shaped segregations and veinlets in the telluride aggregates. The fineness of native gold is 850‰ (Vlasov et al., 2016).

At **the Sentyabr'skoe deposit**, the main tellurides are hessite, altaite, and petzite (Fig. 8*d–h*) (Savva et al., 2016). Also, coloradoite and paratellurite were found (Nikolaev et al., 2013). *Hessite* is deposited in the interstices of comb quartz and forms 0.05–1.50 mm inclusions in chalcopyrite. It is intergrown with altaite and petzite (Fig. 8*d*) and contains a reticulate native-gold aggregate (Fig. 8*e*). *Altaite* forms interstitial inclusions in quartz. It is intergrown with hessite, petzite, native gold, galena, sphalerite, pyrite, and chalcopyrite. The altaite grains are 0.03 to 0.85 mm in size. *Petzite* is present as fine inclusions in altaite and, more seldom, as intergrowths with hessite and native gold. *Coloradoite* is minor and fills the quartz interstices. Its grains vary in size from few to 50 μm. *Paratellurite* (α-TeO_2) forms pseudomorphs after hessite and also occurs as beige crusts along the cracks in ore aggregates. Its segregations measure 10 μm to 1 mm.

MINERAL ASSEMBLAGES AT THE CHUKCHI EPITHERMAL Au–Ag DEPOSITS

Along with the geology and metallogeny of the Chukchi epithermal Au–Ag deposits, of great interest are the mineral composition of their ores and a paragenetic analysis of the minerals. Identification of exotic minerals and study of their segregations and mineral intergrowths yield the main genetic information. The facts established during a detailed mineralogical study of the ore substance and the sequence of formation of mineral assemblages can serve as the basis for constructing geological and genetic models of deposits, classifying their mineral types, and choosing technological schemes for ore dressing and contribute to the development of search criteria. Below, we briefly report the results of mineralogical studies of the Chukchi epithermal Au–Ag deposits. The characteristics of the main mineral assemblages are listed in Table 2.

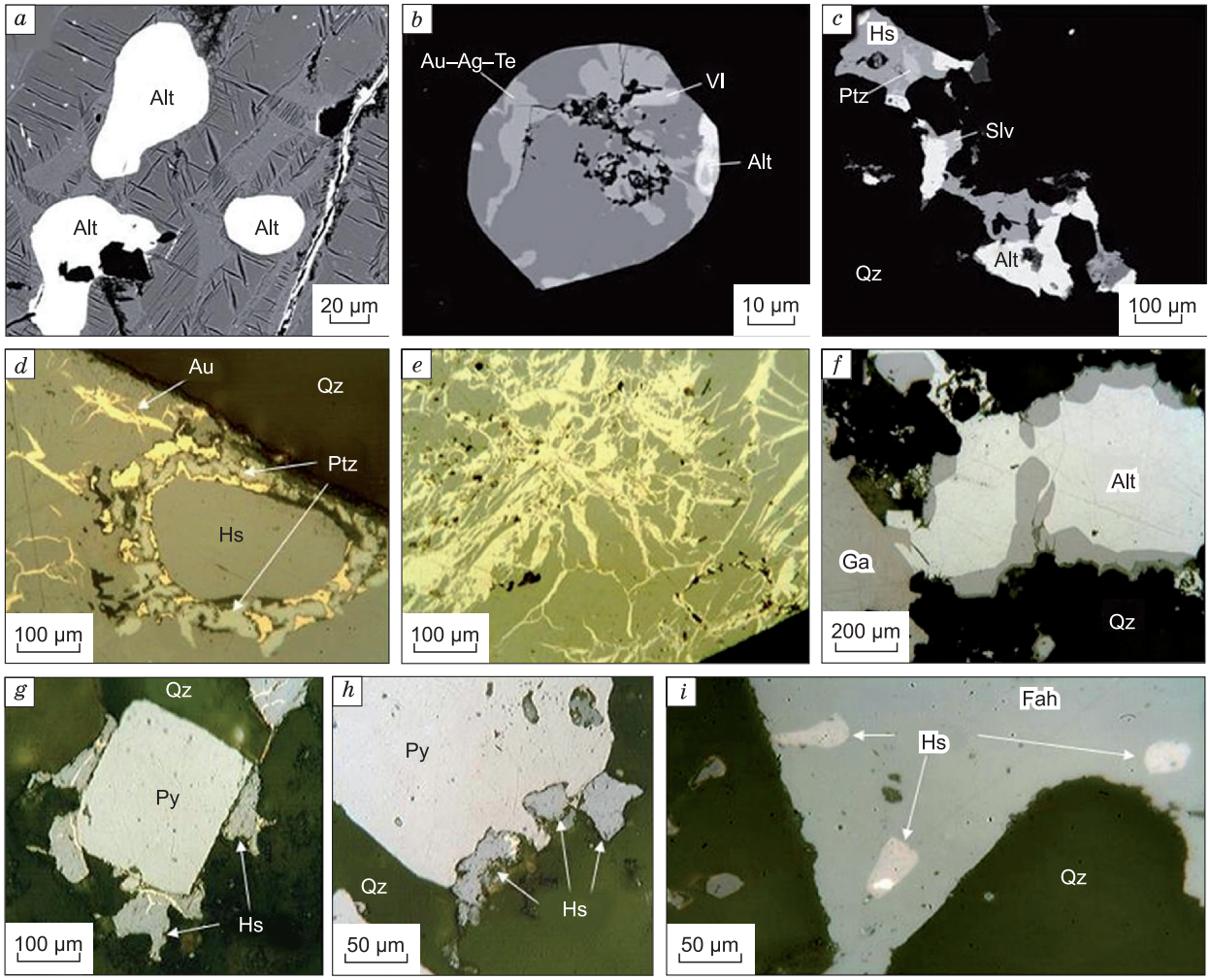

Fig. 8. Telluride mineralization in the ores of the Chukchi epithermal Au–Ag deposits. *a–c* (BSE images), Televeem deposit (Vlasov et al., 2016): *a*, altaite inclusions in disintegrated bornite; *b*, drop-like inclusion (composed of altaite, hessite, unidentified Au–Ag telluride, and volynskite) in bornite; *c*,intergrowth of petzite and sylvanite with hessite and altaite in quartz; *d–h,* Sentyabr'skoe deposit: *d*, *e*, petzite, hessite, and native gold; *f*, intergrowth of altaite and galena; *g*, *h*, intergrowth of hessite and pyrite; *i*, hessite inclusions in fahlore (Dvoinoe deposit). Alt, altaite, Ga, galena, Hs, hessite, Fah, fahlore, Ptz, petzite, Py, pyrite, Slv, sylvanite, Vl, volynskite, Qz, quartz.

The orebodies of **the Corrida deposit** are adularia–quartz veins with abundant pyrite, arsenopyrite, and galena. The productive gold–silver–selenide–acantite paragenesis comprises pyrite, galena, acanthite, Se-sulfosalts, selenides, native silver, Ag sulfides (of the sternbergite–argentopyrite–lenaite series), and native gold with a fineness of 200 to 700‰ (the average is 459‰) (Fig. 5). A specific feature is a significant amount of silver chlorides and bromides of the cerargyrite–embolite–bromyrite series (Kolova et al., 2021).

Within **the Pepenveem ore field**, more than ten zones of secondary coarse-isometric quartzites were revealed (Volkov et al., 2006). The largest of them, the Gigant (Giant) ore zone, extends for 3 km in the northeastern direction (with gaps, up to 5 km) and is 2 km wide in the central part. It comprises three veins and five veinlet–vein and twelve veinlet zones. The Au content varies from 0.2 to 112.3 ppm (the average is 2.7 ppm), and the Ag content, from 20 to 5430 ppm (the average is 594 ppm). Productive gold–silver–sulfosalt paragenesis comprises pyrite, galena, sphalerite, chalcopyrite, minor Cu–Fe silver sulfides (of the lenaite–geffroyite group), fahlores, pyrostylpnite, stephanite, pyrargyrite, polybasite, acanthite, and native gold with a fineness of 597 to 662‰ (the average is 611‰) (Fig. 5).

Within **the Valunistoe ore field**, 12 ore-bearing vein zones were revealed. The best studied are the Glavnaya (Main) and Novaya (New) zones and the Gornyi (Mountainous) site (Zhuravkova et al., 2019; Volkov et al., 2020). Ore mineralization is unevenly distributed in the vein zones, the contents of Au and Ag are within 0–474 and 0–3794 ppm, respectively. The Au/Ag ratio in the veins of the Glavnaya zone varies from 1:5 to 10:1 (Table 2). The productive gold–silver–acanthite paragenesis comprises acanthite, uytenbogaardtite, petrovskaite, naumannite, Au–Ag amalgams, and minerals of the pierceite–polybasite series (Volkov et al., 2020).

Table 2. Characteristics of major mineral types in epithermal Au–Ag deposits of the Chukchi Peninsula

Deposit	Ore structure	Widespread and *rare* ore minerals	Average gold fineness, ‰ Au:Ag	Sulfide content in ores, %	Mineral assemblage (type)
East Chukchi flank zone of the OCVB					
Corrida	Colloform–banded, breccia, veinlet	Pyrite, galena, native gold, Se-acanthite, naumannite Ag *bromides*	459 1:20–1:200	>0.5	Gold–silver– selenide–acanthite
Pepenveem	Colloform spotted, porous, breccia	Pyrite, arsenopyrite, galena, native gold, pearceite, tennantite–tetrahedrite *Lenaite, geffroyite*	611 1:10–1:100	1–2	Gold–silver–sulfosalt
Valunistoe	Colloform–banded, breccia, framework–lamellar	Pyrite, native gold, native silver, galena, chalcopyrite, acanthite, polybasite *Hessite, matildite,* Ag–Hg	608 1:5–1:10	1–2	Gold–silver–acanthite
Inner zone of the OCVB					
Kaienmyvaam	Colloform–banded, veinlet	Pyrite, chalcopyrite, sphalerite, native gold, Se-acanthite, naumannite *Jalpaite, argentopyrite*	600 1:50–1:500	5–7	Gold–silver– selenide–acanthite
Televeem	Colloform–banded, festoon, breccia, veinlet, impregnated	1. Chalcopyrite, polybasite, native gold, galena, acanthite, pearceite *Jalpaite, stromeyerite*	487 1:50–1:200	3–5	Gold–silver–sulfosalt
		2. Hessite, chaclcopyrite, bornite, tetrahedrite, sylvanite, altaite, galena, pyrite *Native tellurium, petzite, hemusite*	1:1–1:10	2–3	Gold–telluride
Central Chukchi sector of the OCVB					
Proval'nye Ozera	Vein–veinlet, spotted, festoon	Hematite, pyrolusite, native gold, naumannite *Polybasite*	600 2:1–1:10	>0.1	Gold–hematite–pyrolusite
Promezhutochnoe	Metacolloidal, banded, breccia, framework–lamellar	Arsenopyrite, pyrrhotite, pyrite, antimonite, berthierite, tetrahedrite, galena, miargyrite *Freieslebenite, löllingite*	703 1:10–1:500	1–2	Gold–arsenopyrite–sulfoantimonite
Kyplatap	Vein–veinlet, spotted, crustification, framework–lamellar	Arsenopyrite, chalcopyrite, electrum, acanthite, fahlores, luzonite, galena, stephanite, *Molybdenite, orpiment?*	570 1:70–1:2200 average 1:450	>0.5	Gold–silver–sulfoarsenide– acanthite
Anadyr' sector of the OCVB					
Kupol	Breccia, colloform–banded, crustification	Native gold, proustite, stephanite, billingsleyite, naumannite, Se-acanthite, chalcopyrite, fahlore, galena *Uytenbogaardtite, fischesserite, billingsleyite*	604 1:20–1:50 average 1:25	>0.5 (up to 10 in the Northern zone)	Gold–silver–acanthite–sulfosalt
Moroshka	Breccia, colloform–banded, crustification	Pyrite, marcasite, arsenopyrite, native gold, sphalerite, proustite, pyrargyrite, stephanite *Pyrostilpnite, selenostephanite, pyrrhotite*	736 1:10–1:15	0.5–1	Gold–silver–sulfosalt
Oloi volcanic belt					
Baimka zone					
Vesennee	Vein–veinlet, banded	Galena, sphalerite, pyrite, magnetite, hematite, Ag-tennantite, chalcopyrite, molybdenite, marcasite, cubanite *Fine native gold in sulfides, native silver, schapbachite, bournonite*	550 1:1–1:17	0.5–1	Gold–silver–polymetallic (associated with porphyry Cu–Mo system)
Early Cretaceous volcanic troughs					
Tytyl'veem volcanic trough					
Dvoinoe	Colloform–banded, veinlet, impregnated	Pyrite, sphalerite, electrum, tetrahedrite, chalcopyrite *Hessite, goldfieldite, cassiterite*	737 1:1–1:0	>0.5	Gold–silver–fahlore
Sentyabr'skoe	Breccia, colloform, veinlet, nest–impregnated, spheroidal	Native gold, pyrite, galena, sphalerite, chalcopyrite *Hessite, petzite, altaite*	801 2:1–10:1	1–3	Gold–polymetallic
Krichal' volcanic trough					
Klen	Colloform–banded, banded, framework–lamellar, breccia, druse	Pyrite, chalcopyrite, native gold, fahlores, pyrargyrite, polybasite, naumannite *Hessite, stromeyerite*	750 1:2–1:5	0.5–2.0	Gold–silver–sulfosalt

Note. Rare ore minerals are italicized.

The Valunistoe deposit is characterized by a wide spread of late vein minerals: calcite, fluorite, and gypsum. Its ores are similar in characteristics to the Au–Ag mineralization of the Kupol deposit but lack complex Au–Ag selenides (Table 2). The sulfides and selenides of the Kupol Au–Ag deposit are associated with native sulfur and jarosite, which indicates highly oxidizing conditions of mineral formation as compared with the Valunistoe deposit.

At **the Televeem deposit**, ores of two main parageneses, gold–sulfosalt and gold–telluride, were revealed (Vlasov et al., 2016). *Gold–sulfosalt ores* were found in adularia–quartz veins in the central part of the deposit. The contents of Au and Ag reach 98 and 113 ppm, respectively. The Au/Ag ratio varies from 1:1 to 1:10; some ore samples contain telluride mineralization. This paragenesis comprises pyrite, low-fineness gold (Fig. 5), minerals of the pierceite–polybasite series, and scarcer chalcopyrite, sphalerite, galena, and Se-acanthite. *Gold–telluride ores* were found on the southwestern flank of the deposit and are quartz–carbonate vein bodies of NW strike. The contents of Au, Ag, and Te in some samples exceed 500, 5000, and 2000 ppm, respectively. This paragenesis comprises bornite, pyrite, chalcopyrite, galena, sphalerite, tetrahedrite-(Zn), spionkopite, native gold, and various tellurium minerals: sylvanite, petzite, altaite, hessite, melonite, volynskite, tellurobismuthite, and native tellurium.

The Sopka Rudnaya and **Promezhutochnoe deposits** are characterized by a significant amount of arsenopyrite and antimonite (Volkov et al., 2006). The silver minerals in the ores are low-fineness native gold, pyrargyrite, proustite, miargyrite, and argentotetrahedrite-(Fe). The minerals inherit the Sb–As signatures of black-shale strata. The Au/Ag ratio in the ores is 1:10–1:500 and lower (Table 2). The sulfide content varies widely depending on the erosional-truncation level. The ores contain gold–arsenopyrite–sulfoantimonite paragenesis (Table 2).

A somewhat different mineral type of Au–Ag deposits (Kyplatap and Kapel'ka) but also with high contents of As and Sb was found on the northwestern flank of the Pegtymel' trough (Petrov and Mikhailov, 1999; Kalko et al., 2014). The degree of ore sulfidation at these deposits is lower than 0.5%. The predominant silver minerals are acanthite, polybasite, often with a Se impurity (up to 2 wt.%), and stephanite. Pyrargyrite, Se-bearing acanthite, low-fineness (315‰) native gold, and native silver are sporadic.

At **the Kupol deposit**, Au–Ag mineralization is concentrated in vein bodies composed of predominant quartz–chalcedony aggregates and sericite and subordinate adularia. The average contents of Au and Ag are 21.5 and 266.6 ppm, respectively. The intrusion of a post-ore dike (Fig. 3) exerted a thermal effect on productive mineralization (Savva et al., 2021). The ores have many specific features, such as a large amount of jarosite in the cement of ore breccias, a low degree of sulfidation (0.5–1.0%), a small amount of adularia, domination of silver sulfide (acanthite) over Ag sulfosalts, and a wide spread of Se-containing minerals. Gold with a fineness of 600–650‰ is the most common (Fig. 5). Although the deposit is formally assigned to the sulfosalt type (Savva et al., 2012), acanthite dominates over sulfosalts in the ores (technological-sampling data), which is typical of thermometamorphosed ores (Savva, 2018).

The mineral composition of the ores of **the Dvoinoe deposit** is not diverse, and the mineral segregations are small and intimately intergrown with each other, which indicate steeply gradient conditions of the deposit formation. The ores are poor in silver minerals (hessite and extremely scarce acanthite). The main paragenesis of the ores is gold–silver–fahlore (Table 2). Early gold-bearing pyrite was sheared to different degrees, from small cracks to fine clastics, and cemented with intimately intergrown polysulfide minerals (Volkov et al., 2018).

At **the Sentyabr'skoe deposit**, gold–polysulfide mineralization was explored by boreholes to a depth of more than 250 m (Fig. 3). The content of Au in the ores varies from 6 to 400 ppm, and Au/Ag is 2:1–10:1, i.e., gold dominates over silver. Massive and nest mineralization occurs as lenticular veinlets with swells in the breccia cement, and disseminated sulfide mineralization is developed at the edges of metasomatized clastics. The ores contain gold–polysulfide paragenesis with tellurides (Savva et al., 2016).

The ore bodies of **the Vesennee deposit** with Au–Ag mineralization are 0.5–3.0 m thick quartz–carbonate medium-sulfide veins and 10–150 m thick and 500–1200 m long veinlet zones forming a large stockwork (~1 km^2). The gold–silver–polymetallic paragenesis comprises As-bearing pyrite, sphalerite, galena, chalcopyrite, tetrahedrite-(Zn) (with up to 4 wt.% Ag), acanthite, native gold (with a fineness of 660–840‰), hessite, and Ag-sulfosalts (pierceite–polybasite) (Nikolaev et al., 2020).

The ore bodies of **the Klen deposit** are quartz–adularia and quartz–carbonate veins accompanied by a series of tongues (smaller veins and veinlet zones). The length of major commercial veins No. 1 and No. 2 is 1700–1250 m along the strike and up to 500 m along the dip. The veins are steeply dipping (50–80°). The average thicknesses of vein No. 1 and vein No. 2 are 5.1 and 1.2 m, respectively. The average content of Au in the orebodies is 17.4 ppm, and the average content of Ag is 25.6 ppm. The main gold–silver–sulfosalt paragenesis comprises pyrite, chalcopyrite, sphalerite, galena, tetrahedrite, Se-polybasite, acanthite, pyrargyrite, and native gold (with a fineness of 630–800‰). Hessite, stromeyerite, and naumannite are scarce. The main specific features are the abundance of polybasite, including a Se-containing one, the presence of pyrargyrite, and the absence of arsenopyrite and antimonite (Nikolaev et al., 2020).

RESULTS OF STUDY OF FLUID INCLUSIONS

Fluid inclusions (FIs) were thoroughly studied by microthermometry in auriferous quartz of epithermal Se- and Te-type Au–Ag mineralization at 14 deposits of volcanic belts

on the Chukchi Peninsula (Volkov and Prokof'ev, 2011; Volkov et al., 2012, 2018, 2019, 2021; Nikolaev et al., 2013, 2016, 2020; Kalko et al., 2014; Vlasov et al., 2016; Prokofiev et al., 2019a, b; Kolova et al., 2021).

Numerous fluid inclusions larger than 10 μm were found mainly in auriferous quartz from gold ores, which has grains of different textures (pectinate, feathered, or radiolithic) and formed synchronously with adularia, as evidenced by the surfaces of synchronous growth.

A microscopic study at room temperature revealed two types of FIs in the quartz: (1) vapor-rich inclusions containing a vapor bubble with a rim of an aqueous solution (Fig. 9*a*) and (2) two-phase inclusions consisting of an aqueous solution and a vapor bubble occupying 5–20% of the

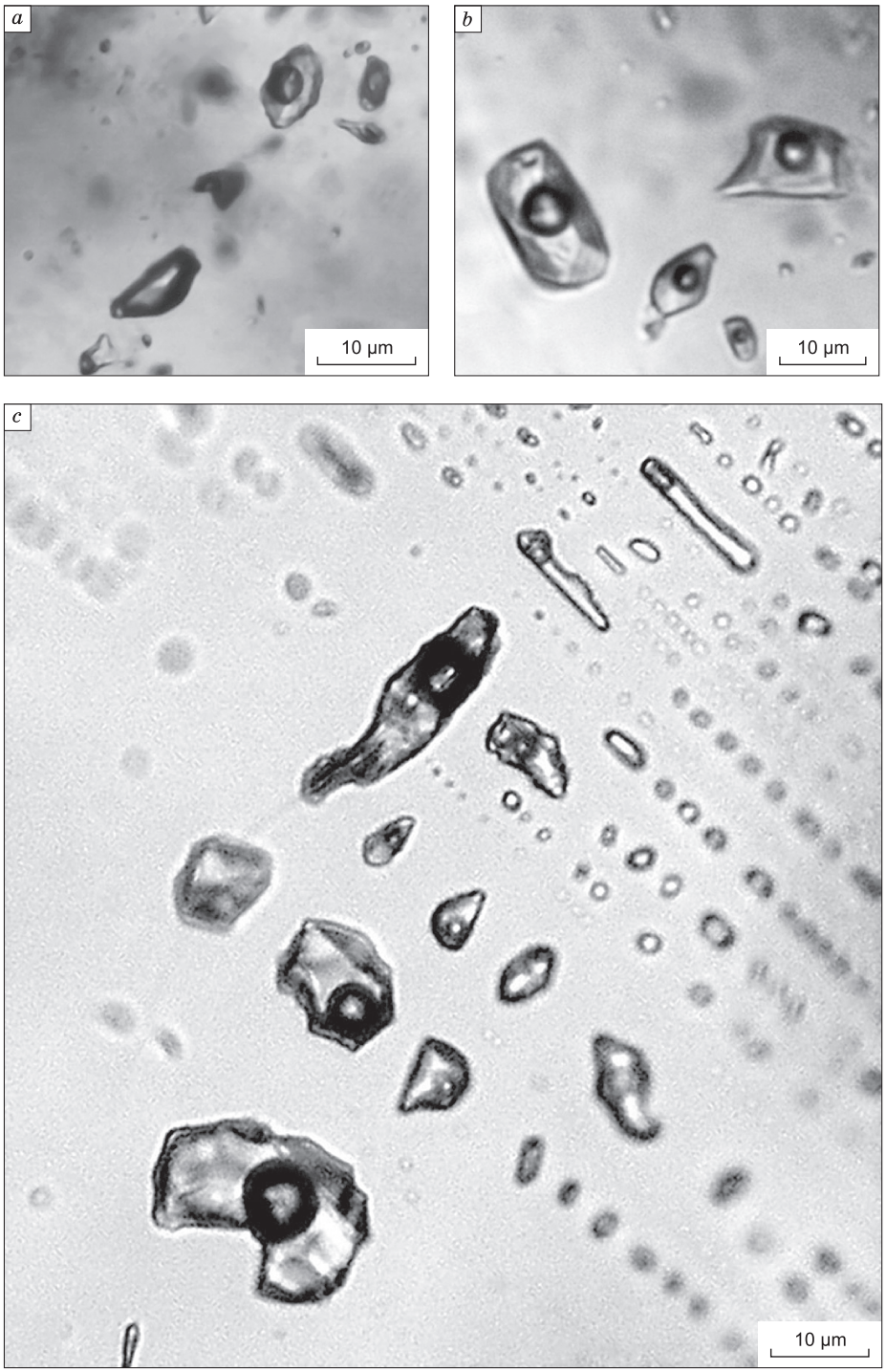

Fig. 9. Typical fluid inclusions in quartz from epithermal Au–Ag deposits of the Chukchi volcanic belts. *a*, Association of essentially gas and water–salt inclusions in quartz from the Zhil'noe deposit, which testifies to the heterogeneous state of the fluid; *b*, two-phase inclusions evenly distributed in quartz from the Kaienmyvaam deposit; *c*, primary two-phase inclusions in quartz from the Promezhutochnoe deposit.

inclusion volume (Fig. 9*b*, *c*). Type 1 FIs found in early quartz from adularia–quartz veins are localized in the same zones or cracks as type 2 FIs, forming a single association. This indicates a heterogeneous state (boiling-up) of the mineral-forming fluid in certain periods of hydrothermal activity. Most of type 2 FIs are filled with water vapor. Sometimes, cooling of type 2 FIs led to condensation of carbon dioxide, which homogenized into a gas on heating. Type 1 FIs not accompanied by type 2 ones usually occur in later quartz.

The highest homogenization temperatures were measured for boiling-up heterogeneous fluids. Therefore, to estimate the crystallization temperatures, no correction for the influence of pressure is required (Roedder, 1984).

According to the trapping time, the found FIs are subdivided into (i) primary, present in the growth zones (Fig. 9*c*) or evenly distributed throughout the quartz grains (Fig. 9*b*), (ii) primary–secondary, localized in the inner quartz cracks, and (iii) secondary, confined to cross cracks. For micro thermometric studies, we chose mainly primary FIs. For completeness, we also examined primary–secondary and secondary inclusions.

Micro thermometric studies of FIs were carried out in the Laboratory of Geochemistry of the Institute of Geology of Ore Deposits, Petrography, Mineralogy and Geochemistry, Moscow, using a measuring system comprising a THMSG-600 (Linkam, England) heating micro stage, an Olimpus microscope (Japan), a video camera, and a control computer. This system provides a real-time measurement of phase transition temperatures in the interval from –196 to 600 ºC, control over them at high magnifications, and obtaining of digital photomicrographs.

Individual FIs were studied in doubly polished 0.3–0.5 mm thick quartz plates. After microscopic examination and photography, the preparations were taken off the glass and washed with ethyl alcohol. Then, the pieces of quartz with inclusions for study were mechanically separated. The salt concentration in the inclusions was calculated from the melting point of ice, using the data from Bodnar and Vityk (1994). The pressure in associations of syngenetic type 1 and type 2 FIs in a heterogeneous fluid was estimated as the pressure of saturated water vapor. Sometimes, carbon dioxide condensed in type 2 FIs during cooling. In this case, its density was estimated from the homogenization temperature of the CO_2 phase, and the total pressure was estimated as the sum of the partial pressures of CO_2 and H_2O. The salt concentrations and the densities and pressures of water vapor and CO_2 were estimated using the FLINCOR program (Brown, 1989).

The bulk composition of fluids in inclusions from productive quartz from different deposits was analyzed in 0.7 g samples of the quartz fractions of –0.5 to +0.25 mm at the Central Research Institute of Geological Prospecting for Base and Precious Metals (TsNIGRI), Moscow (analyst Yu.V. Vasyuta), following the earlier proposed technique (Kryazhev et al., 2006). The inclusions in quartz were unsealed at 500 ºC.

The content of water was determined by gas chromatography (TsVET-100 chromatograph) for calculation of the element concentrations in the hydrothermal solution. Also, analyses for carbon dioxide and methane were carried out.

After the preparation of aqueous extracts, the concentrations of Cl^-, HCO_3^-, and SO_4^{2-} in the solution were determined by ion chromatography (TsVET-3006 chromatograph, sensitivity of 0.01 mg/L), and the concentrations of K, Na, and Rb, by ICP MS (Elan-6100 mass spectrometer).

The results of microthermometric studies of more than 1500 FIs in quartz and other minerals from the ores of the Chukchi epithermal gold deposits are presented in Table 3 and in Fig. 10. The determined chemical composition of fluids is given in Table 4. The parameters and composition of fluids from the deposits of different regions of the Chukchi Peninsula are generally similar, but there are some differences.

The homogenization temperatures of inclusions of mineral-forming fluids at the deposits of the East Chukchi flank zone of the OCVB vary from 163 to 350 °C, the fluid salinity is 0.2–3.6 wt.% NaCl equiv., and the fluid density is 0.56–0.90 g/cm^3.

The fluid pressure reaches 80–160 bars. The fluids contain (g/kg of water) CO_2 (2–179), CH_4 (0.1–4.2), Cl^- (0–9.5), HCO_3^- (0–136), SO_4^{2-} (0–79), Na^+ (0.6–17), and K^+ (0.1–80). The main geochemical indices of the fluid are as follows: CO_2/CH_4 = 9–463, Na/K = 0.05–5.9, and K/Rb = 133–2363.

The homogenization temperatures of inclusions of mineral-forming fluids at the deposits of the inner zone of the OCVB range from 136 to 327 °C, the fluid salinity is low (0.2–1.6 wt.% NaCl equiv.), and the fluid density varies from 0.63 to 0.94 g/cm^3. The fluid pressure is estimated at 30–120 bars. The mineral-forming fluids contain (g/kg of water) CO_2 (14–762), CH_4 (0.1–3.5), Cl^- (6–96), HCO_3^- (1.1–40), SO_4^{2-} (1.5–53), Na^+ (3.7–32), and K^+ (0.4–58). The main geochemical indices of the fluid are as follows: CO_2/CH_4 = 28–2018, Na/K = 0.4–10.5, and K/Rb = 324–2435.

The homogenization temperatures of inclusions containing mineral-forming fluids in quartz from the deposits of the Central Chukchi sector of the OCVB vary from 142 to 353 °C, the fluid salinity reaches 0.2–4.3 wt.% NaCl equiv., and the fluid density is within 0.58–0.93 g/cm^3. The fluid pressure varies from 150 to 250 bars. The hydrothermal fluids contain (g/kg of water) CO_2 (0.3–59), CH_4 (0.02–3.20), Cl^- (0–9.9), HCO_3^- (4.7–36.4), SO_4^{2-} (0–21), Na^+ (0.48–24.0), and K^+ (0.13–19.0). The main geochemical indices of the fluid are as follows: CO_2/CH_4 = 15.4–143.0, Na/K = 0.9–3.9, and K/Rb = 291–911.

The homogenization temperatures of inclusions of mineral-forming fluids at the epithermal deposits of the Oloi volcanic belt (Vesennee deposit) range from 156 to 404 °C, the fluid salinity is estimated at 1.2–22.9 wt.% NaCl equiv., and the fluid density is 0.70–0.94 g/cm^3. The ore-forming fluids contain (g/kg of water) CO_2 (7–31), CH_4 (0.25–0.40), Cl^- (6.7–15.0), HCO_3^- (0–16.6), SO_4^{2-} (4.4–9.0), Na^+ (0.6–16.0),

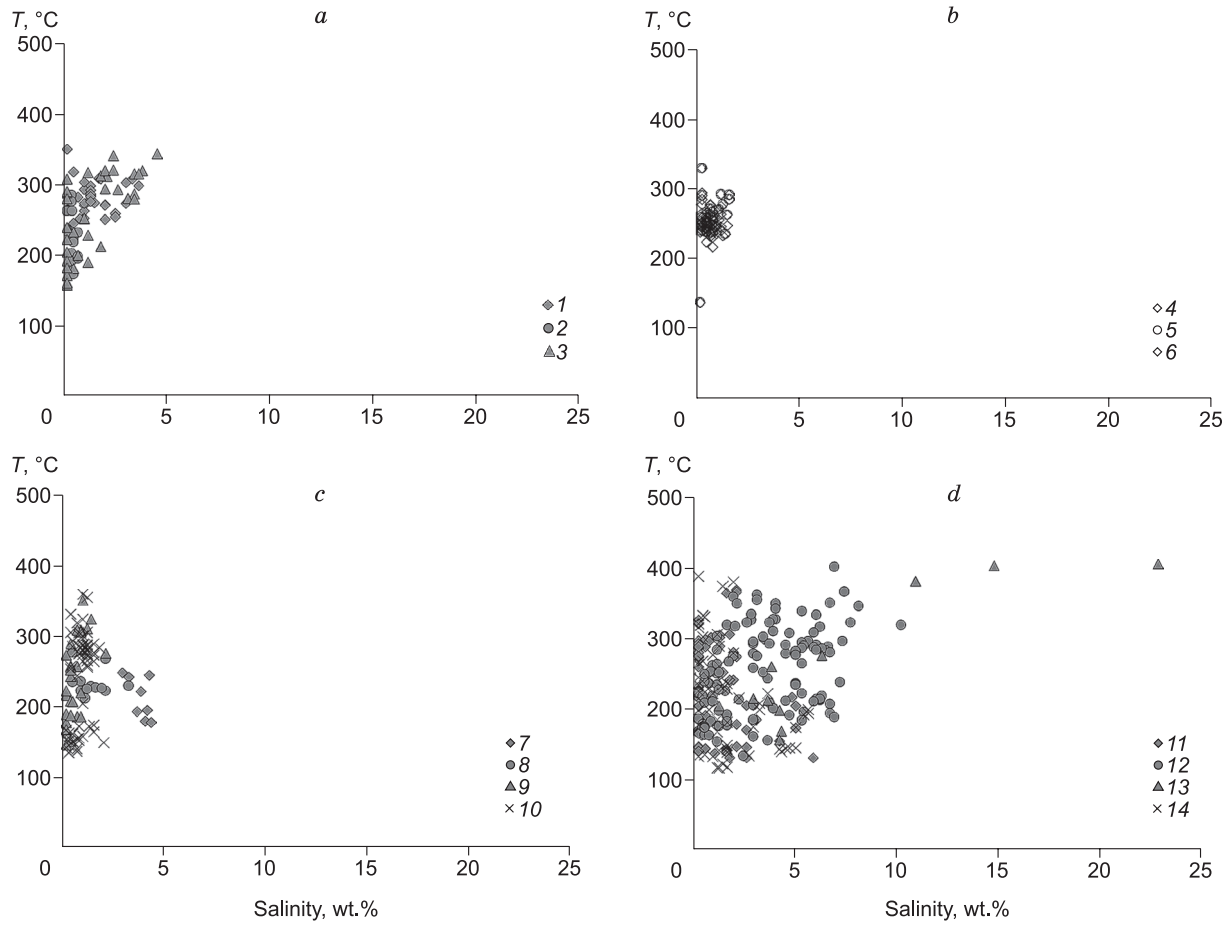

Fig. 10. Temperature vs. salinity of mineral-forming fluids of epithermal Au–Ag mineralization of the Chukchi volcanic belts. *a*, East Chukchi flank zone of the OCVB; *b*, inner zone of the OCVB; *c*, Central Chukchi sector of the OCVB; *d*, Oloi volcanic belt (Baimka zone) and Early Cretaceous Tytel'vevem and Krichal' volcanic troughs. Deposits: *1*, Zhil'noe, *2*, Valunistoe; *3*, Erguveem; *4*, Arykevaam; *5*, Televeem; *6*, Kaienyvaam; *7,* Promezhutochnoe; *8*, Kupol; *9*, Kapel'ka; *10*, Uteveem; *11*, Dvoinoe; *12*, Sentyabr'skoe; *13*, Vesennee, *14*, Klen.

and K^+ (0.8). The main geochemical indices of the fluid are as follows: CO_2/CH_4 = 29–78, Na/K = 0.7–20.0, and K/Rb = 324–345.

The homogenization temperatures of inclusions of mineral-forming fluids at the epithermal deposits of the Early Cretaceous volcanic troughs (Tytel'veem and Krichal') vary from 110 to 390 °C, the fluid salinity is estimated at 0.2–8.1 wt.% NaCl equiv., and the fluid density reaches 0.48–0.94 g/cm^3. The fluid pressure is the highest, 80 to 570 bars. The ore-forming fluids contain (g/kg of water) CO_2 (1.3–70.0), CH_4 (0.02–1.1), Cl^- (0.1–11.0), HCO_3^- (0–11.9), SO_4^{2-} (0–0.8), Na^+ (0–7.1), and K^+ (0.1–2.0). The main geochemical indices of the fluid are as follows: CO_2/CH_4 = 13–409, Na/K = 1.1–16.0, and K/Rb = 202–2722.

DISCUSSION AND CONCLUSIONS

The mineralogical specifics of the Chukchi epithermal Au–Ag deposits are determined by the areas of volcanism of different ages and compositions, whose products are concentrated in volcanic belts superposed on the independently evolved geologic blocks (terranes) that make up the folded basement of the OCVB and differ in rock composition (Sidorov et al., 2009). The substance transported from the basement rocks determines the mineralogical and geochemical features of the ores and clarifies the causes of the diversity of the mineralogical and geochemical types of epithermal Au–Ag mineralization within the volcanic belts.

The high contents of As and Se in the epithermal Au–Ag ores of the deposits were probably inherited from the As- and Se-enriched black-shale flysch sequences of the basement of volcanic structures (Savva, 2005; Volkov et al., 2006). The mineral composition of the ores was significantly governed by the deeply metamorphosed rocks of the belt basement (As and Sb were supplied to the ores from the Eskimo massif in the East Chukchi sector, and Cl, F, and Br, from the buried seawater) and by the intrusive rocks of dome structures with certain geochemical signatures (Cu–Mo, Sn–W, and Bi–Te), which also contributed to the supply of components to the ores.

Table 3. Parameters of ore-forming fluids of the Chukchi epithermal Au–Ag deposits

Deposit, region	Physicochemical parameters of fluids					Reference
	T, °C	C*, wt.%	*d*, g/cm^3	*P*, bars	Composition**	
East Chukchi flank zone of the OCVB						
Zhil'noe	246–350 (233)	0.2–3.6	0.56–0.81	80–160 (42)	H_2O	(Elmanov et al., 2018)
Valunistoe	174–284 (121)	0.2–0.7	0.73–0.90	–	H_2O	(Volkov et al., 2019)
Corrida	163–340 (58)	0.2–3.6	0.63–0.90	108–140 (3)	H_2O	(Kolova et al., 2021)
Inner zone of the OCVB						
Arykevaam	234–267 (78)	0.4–1.2	0.79–0.82	–	H_2O	(Volkov et al., 2012)
Televeem	136–327 (130)	0.2–1.6	0.63–0.94	30–120 (27)	H_2O	(Vlasov et al., 2016)
Kaienmyvaam	215–292 (250)	0.3–1.3	0.71–0.85	30–70 (55)	H_2O	(Prokofiev et al., 2019b)
Central Chukchi sector of the OCVB						
Promezhutochnoe	180–250 (8)	2.9–4.3	0.83–0.92	250 (1)	H_2O, CO_2+H_2O	(Volkov and Prokof'ev, 2011)
Kupol	211–276 (59)	0.5–3.2	0.75–0.86	–	H_2O	(Volkov et al., 2012)
Kapel'ka	142–353 (310)	0.2–2.1	0.58–0.93	150–160 (12)	H_2O	(Kalko et al., 2014)
Uteveem	142–353 (33)	0.2–1.2	0.59–0.93	160 (5)	H_2O	(Prokofiev et al., 2019a)
Oloi volcanic belt						
Baimka zone						
Vesennee	156–404 (66)	1.2–22.9	0.70–0.94	–	H_2O	(Nikolaev et al., 2016)
Early Cretaceous volcanic troughs						
Tytyl'veem trough						
Dvoinoe	153–320 (137)	0.2–5.9	0.55–0.93	–	H_2O	(Volkov et al., 2018)
Sentyabr'skoe	155–360 (27)	0.9–8.1	0.67–0.94	80–570 (8)	H_2O, CO_2+H_2O	(Nikolaev et al., 2013)
Krichal' trough						
Klen	110–390 (176)	0.2–5.6	0.48–0.91	–	H_2O	(Nikolaev et al., 2020)

Note. Parenthesized is the number of determinations.
* Fluid salinity, wt.% NaCl equiv..
** Composition of the gas phase of fluid inclusions.

In volcanoplutonic edifices, the composition of minerals and their intergrowths is strongly influenced by the thermal metamorphism of volcanic ores and the associated redistribution of ore substance (Savva, 2018). The degree of ore metamorphism is a crucial indicator of the deposit reserves. The processes leading to the thermal metamorphism of ores are accompanied by powerful energy pulses and favor the redistribution of ore metals. The differentiation and local concentration of gold and silver, related to thermal and dynamothermal metamorphism, can be considered a natural enrichment of ores, which ultimately affects their mineral type (Savva, 2018).

The results of mineralogical studies show that most of the Chukchi epithermal Au–Ag deposits (Kupol, Corrida, etc.) can be assigned to the Se type (Table 1). The ores of some of them (Valunistoe, Dvoinoe, etc.) contain both Se- and Te-bearing minerals (Table 1). At the same time, tellurides are considered exotic at these deposits (Nikolaev et al., 2013; Savva et al., 2016; Vlasov et al., 2016). Usually, the most telluride-enriched sites of the deposits are located on the flanks, at some distance from the main Au–Ag ores, e.g., in the south of the deposit (Sentyabr'skoe) or in the southeast (Televeem). According to Shikazono et al. (1990), Te mineralization is deposited at a higher level of the epithermal system than Se mineralization. Since Se and Te are trace elements, their extraction as by-products from the ores of epithermal deposits is inexpedient.

Based on the mineral types of ores of the Chukchi epithermal Au–Ag deposits, we have drawn the following conclusions:

– the gold–silver–acantite type testifies to the ore metamorphism and redistribution of Au and Ag in the ores (natural enrichment) (Kupol and Corrida deposits);

– the gold–silver–telluride paragenesis is evident of the supply of Te by late magmatic injections (Sentyabr'skoe and Televeem deposits);

– the wide spread of copper minerals indicates the relationship of the deposit with a porphyry Cu system (Vesennee and Televeem deposits);

– the large number of breccia structures points to the unstable tectonic setting of the deposit formation (Kupol, Promezhutochnoe, and other deposits);

– the low sulfide content indicates high enrichability of the ores (Dvoinoe deposit).

The mineral-forming fluids of the Chukchi Au–Ag deposits have many common features that permit these depos-

Table 4. Major components of mineral-forming fluids at epithermal deposits of northeastern Russia (g/kg of solution)

Deposit	CO_2	CH_4	Cl^-	HCO_3^-	SO_4^{2-}	Na^+	K^+	Salinity, wt.%	CO_2/CH_4	Na/K	K/Rb	Reference
East Chukchi flank zone of the OCVB												
Zhil'noe	4–7	0.1–0.7	0.2–2.0	0.8–7.0	0–79	1.4–9.7	1.8–38	1.1–13.2	9.7–51.8	0.26–0.76	133–2363	(Elmanov et al., 2018)
Valunistoe	1.8–7	0.1–0.6	1.6–5.2	–	0–2.1	0.6–2.3	0.1–0.7	0.2–0.8	9.3–30.3	1.1–5.9	478–3901	(Our data)
Valunistoe	5	0.07	–	–	3.1	2.3	0.9	0.4	77	0.4	239	(Volkov et al., 2020)
Corrida	12–179	0.15–4.2	0.1–9.5	9.4–136	1.3–35	2.1–17	1.8–80	3.1–25.7	62–463	0.05–3.1	315–2230	(Our data)
Inner zone of the OCVB												
Arykevaam	218–726	0.1–2.3	6–20	2.4–14.7	16–20	3.7–5.8	1.8–10	4.5–6.1	315–2818	0.4–3.2	324–743	(Volkov et al., 2020)
Televeem	14	0.70	6.6	1.1	1.5	4.2	0.4	1.5	28.1	10.5	1290	(Our data)
Kaienmyvaam	290–762	1.4–3.5	49–96	1.9–40	5.3–53	10–32	2.5–58	8.8–25.9	91–552	0.5–4.0	356–2435	(Our data)
Central Chukchi sector of the OCVB												
Promezhu-tochnoe	0.3	0.02	0.23	4.7	–	0.48	0.13	3.0	18.5	3.6	1114	(Volkov and Prokof'ev, 2011)
Kupol	2–59	0.02–3.2	0–0.15	6.6–117	1.3–21	1.6–24	0.8–19	1.1–19.9	18–143	1.3–3.9	291–911	(Our data)
Kapel'ka	16	1.05	9.9	36.4	–	4.0	4.4	6.6	15.4	0.9	518	(Our data)
Oloi volcanic belt												
Baimka zone												
Vesennee	7–31	0.25–0.40	6.7–15	0–16.6	4.4–9.0	0.6–16	0.8	1.3–6.0	29–78	0.7–20	324–345	(Our data)
Early Cretaceous volcanic troughs												
Tytyl'veem trough												
Dvoinoe	1.3–5	0.02–0.13	0.1–1.5	4.6–11.9	0.2–0.8	1.4–2.8	0.3–1.4	0.2–1.8	34–217	1.4–5.0	202–2722	(Our data)
Sentyabr'skoe	5–70	0.03–1.1	0.15–11	0.02–2.1	–	0.2–5.2	0.1–1.2	0.1–1.9	61–409	1.1–5.9	240–704	(Our data)
Krichal' trough												
Klen	11–28	0.05–0.29	0.35–2.2	0–0.8	–	0–7.1	1.7–2.0	0.1–1.7	13–37	1.2–16	597	(Our data)

its to be considered epithermal LS ones (Simmons et al., 2005): low and moderate temperatures, low salinity, a heterogeneous state at the early stages of the hydrothermal process (Table 4), domination of carbon dioxide over methane, and the presence of Cl^-, HCO_3^-, SO_4^{2-}, K^+, Na^+, and Rb^+ in different proportions.

There are, however, some differences in the physicochemical parameters and chemical composition of mineral-forming fluids in different regions of the Chukchi Peninsula (Tables 3 and 4; Fig. 10). The maximum temperatures and salinities are specific to fluids in the Central Chukchi sector of the OCVB and in the Oloi volcanic belt of the Baimka zone, and the minimum ones are typical of fluids in the East Chukchi flank zone and inner zone of the OCVB. The fluids of the latter zones are also enriched in SO_4^{2-}. The maximum pressure has been established for fluids at the Sentyabr'skoe deposit in the Central Chukchi sector of the OCVB. The salinity of mineral-forming fluids in the inner zone of the OCVB is, on average, half that of fluids in the East Chukchi flank zone of the belt, but the content of sulfates is higher. At the same time, the fluids in the inner zone of the OCVB are richer in CO_2 and HCO_3^- than the fluids in the East Chukchi flank zone of the belt.

The K/Rb ratio in the fluids varies from 133 to 2722. The low values of the ratio (<250 (Irber, 1999)) suggest the participation of magmatic fluids in the ore process, and the high values (>250) indicate the interaction of a hydrothermal fluid with the host rocks, accompanied by the loss of Rb. Undoubtedly, meteoric waters were also involved in the ore-forming process, which was favored by the shallow depth of ore deposition and the presence of open tectonic fractures.

For a correct comparison of the large arrays of numerical data on the fluid parameters, we used box plots (Fig. 11). They show that the maximum temperature and salinity of fluids increase in passing from the inner zone of the OCVB to the Oloi volcanic belt. The changes in average tempera-

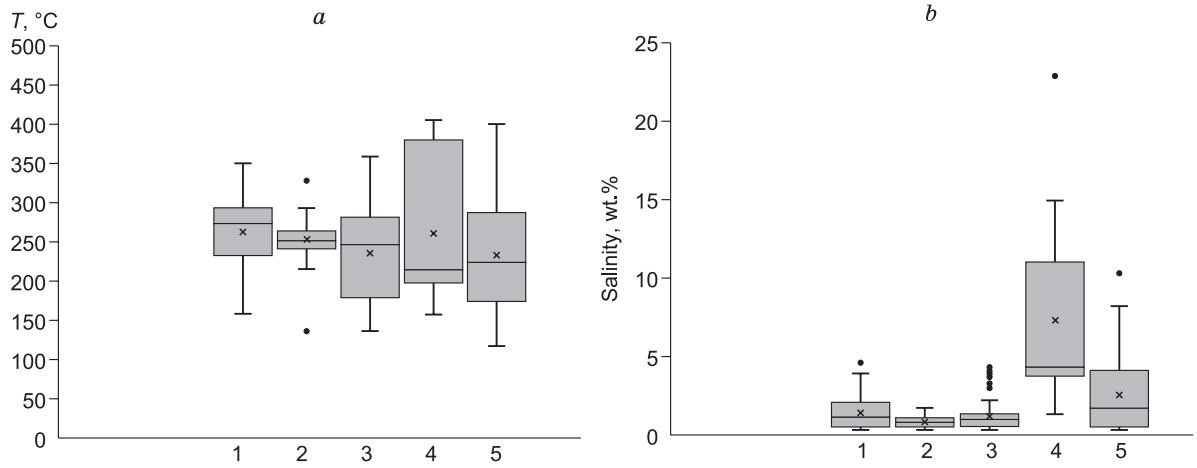

Fig. 11. Box plots of the homogenization temperatures (*a*) and fluid salinity (*b*) of inclusions in minerals of epithermal Au–Ag deposits in northeastern Russia. Line inside the box is a median, cross is the average value, and points mark outliers. Regions: 1, East Chukchi flank zone of the OCVB; 2, inner zone of the OCVB; 3, Central Chukchi sector of the OCVB; 4, Oloi volcanic belt, Baimka zone (Vesennee deposit); 5, Early Cretaceous volcanic troughs (Tytel'veem and Krichal').

tures show a reverse tendency, which might be due to the maximum condensation at the deposits that are the most distant from magma chambers.

Probably, the physical state of fluids at the beginning of ore deposition is related to the location of the ore deposition area relative to magma chambers. At the maximum distance from the chambers (fluids of the East Chukchi flank zone and inner zone of the OCVB), the vapor fluid might have undergone condensation. This might be the cause of the low salinity of the fluids that formed ore deposits in these areas, of the maximum contents of sulfates, bicarbonates, and carbon dioxide, and of the enrichment of the ores in some trace elements that can be transferred with the gas phase. At the same time, the deposits of the Central Chukchi sector of the OCVB and the Baimka zone of the OVB formed with the active participation of magmatic fluids in the state of a liquid aqueous solution. This is indicated by the high salinity of the deposit fluids, which reaches a maximum in the fluids from the Vesennee deposit in the Baimka zone, where magmatogene porphyry deposits occur. The above model of the deposit formation might explain the observed differences in the parameters and composition of mineral-forming fluids in different regions of the Chukchi Peninsula.

The fluid inclusion data permit us to regard the Vesennee deposit (Baimka zone of the OVB) as an epithermal IS one and to predict the discovery of HS deposits in the inner zone of the OCVB.

The work was supported by grant 13.1902.21.008 from the Ministry of Science and Higher Education of the Russian Federation.

REFERENCES

Akinin, V.V., 2012. Late Mesozoic and Cenozoic Magmatism and Transformation of the Lower Crust in the North Pacific Framing. ScD Thesis [in Russian]. IGEM RAN, Moscow.

Akinin, V.V., Tomson, B.T., Polzunenkov, G.O., 2015. U–Pb and $^{40}Ar/^{39}Ar$ dating of magmatism and mineralization at the Kupol and Dvoinoe gold deposits, in: Isotope Dating of Geologic Processes: New Results, Approaches, and Prospects. Proceedings of the Sixth Russian Conference on Isotope Geochronology [in Russian]. IGGD RAN, St. Petersburg, pp. 19–21.

Belousov P.E., Vol'fson A.A., Volkov A.V., Sidorov A.A., Murashov K.Yu., Galyamov A.L., Sidorova N.V., 2020. Argillizite "hats" of Kompleksnoe ore occurrence in Kayenmyvaam volcanic uplift (central Chukotka). J. Volcanol. Seismol. 14 (5), 283–291, doi: 10.1134/S0742046320050024.

Belyi, V.F., 1994. Geology of the Okhotsk–Chukchi Volcanic Belt [in Russian]. SVKNII DVO RAN, Magadan.

Belyi, V.F., Sidorov, A.A., Volkov, A.V., Vashchilov, Yu.Ya., 2008. The structure and evolution of the Kaiemraveem volcanic field: A new ore field in the Chukchi Peninsula. J. Volcanol. Seismol. 2 (3), 149–157.

Bindi, L., Pingitore, N.E., 2013. On the symmetry and crystal structure of aguilarite, Ag_4SeS. Mineral. Mag. 77 (1), 21–31, doi: 10.1180/minmag.2013.077.1.03.

Bodnar, R.J., Vityk, M.O., 1994. Interpretation of microthermometric data for H_2O–NaCl fluid inclusions, in: Fluid Inclusions in Minerals: Methods and Applications: Short Course of the Working Group (IMA) "Inclusions in Minerals", Pontignano, Siena, 1–4 September 1994. Blacksburg, VA, Virginia Tech, pp. 117–130.

Bortnikov, N.S., 2006. Geochemistry and origin of the ore-forming fluids in hydrothermal–magmatic systems in tectonically active zones. Geol. Ore Deposits 48 (1), 1–22, doi: 10.1134/S1075701506010016.

Bortnikov, N.S., Lobanov, K.V., Volkov, A.V., Galyamov, A.L., Vikent'ev, I.V., Tarasov, N.N., Distler, V.V., Lalomov, A.V., Aristov, V.V., Murashov, K.Yu., Chizhova, I.A., Chefranov, R.M., 2015. Strategic metal deposits of the Arctic Zone. Geol. Ore Deposits 57 (6), 433–453, doi: 10.1134/S1075701515060021.

Bortnikov, N.S., Volkov, A.V., Galyamov, A.L., Vikent'ev, I.V., Aristov, V.V., Lalomov, A.V., Murashov, K.Yu., 2016. Mineral resources of high-tech metals in Russia: State of the art and outlook. Geol. Ore Deposits 58 (2), 83–103, doi: 10.1134/S1075701516020021.

Brown, P., 1989. FLINCOR: a computer program for the reduction and investigation of fluid inclusion data. Am. Mineral. 74 (11–12), 1390–1393.

Elmanov, A.A., Prokofiev, V.Yu., Volkov, A.V., Sidorov, A.A., Voskresenskiy, K.I., 2018. First data on formation conditions of the Zhilnoye

Au–Ag epithermal gold deposit (Eastern Chukotka, Russia). Dokl. Earth Sci. 480 (2), 725–729, doi: 10.1134/S1028334X18060247.

Firsov, L.V., 1980. Gold–Quartz Formation of the Yana–Kolyma Belt [in Russian]. Nauka, Novosibirsk.

Hedenquist, J.W., Arribas, A., Gonzalez-Urien, E., 2000. Exploration for epithermal gold deposits, in: Gold in 2000. Reviews in Economic Geology. Society of Economic Geologists, Littleton, pp. 245–277.

Irber, W., 1999. The lanthanide tetrad effect and its correlation with K/Rb, Eu/Eu*, Sr/Eu, Y/Ho, and Zr/Hf of evolving peraluminous granite suites. Geochim. Cosmochim. Acta 63 (3–4), 489–508, doi: 10.1016/S0016-7037(99)00027-7.

Kalko, I., Vlasov, E., Prokofiev, V., Nikolaev, Yu., Sidorina, Yu., Bugaev, I., Usenko, V., 2014. The Kapelka silver prospect: geochemical structure and characteristics of ore forming process, in: Geoconference on Science and Technologies in Geology, Exploration and Mining: 14th International Multidisciplinary Scientific Geoconference SGEM 2014, 17–26 June, 2014, Albena, BulgariaSTEF92 Technology, Sofia, Book 1, Vol. 1, pp. 333–340.

Khanchuk, A.I. (Ed.), 2006. Geodynamics, Magmatism, and Metallogeny of Eastern Russia [in Russian]. Dal'nauka, Vladivostok, Books 1 and 2.

Kolova, E.E., Savva, N.E., Zhuravkova, T.V., Glukhov, A.N., Palyanova, G.A., 2021. Au–Ag–S–Se–Cl–Br mineralization at the Corrida deposit (Russia) and physicochemical conditions of ore formation. Minerals 11 (2), 144, doi: 10.3390/min11020144.

Kovalenker, V.A., Plotinskaya, O.Yu., 2005. Te and Se mineralogy of Ozernovskoe and Prasolovskoe epithermal gold deposits (Kuril–Kamchatka volcanic belt). Geochem. Mineral. Petrol. 43, 118–124.

Kryazhev, S.G., Prokofiev, V.Yu., Vasyuta, Yu.V., 2006. Application of ICP MS on analysis of the composition of ore-forming fluids. Vestnik Moskovskogo Universiteta, Ser. 4. Geol., No. 4, 30–36.

Ledneva, G.V., Pease, V.L., Bazylev, B.A., 2016. Late Triassic siliceous-volcano-terrigenous deposits of the Chukchi Peninsula: composition of igneous rocks, U–Pb age of zircons, and geodynamic interpretations. Russ. Geol. Geophys. 57 (8), 1119–1134, doi: 10.1016/j.rgg.2016.08.001.

Lindgren, W., 1933. Mineral Deposits. McGraw-Hill Book Company, New York.

Lorentz, D.A., Sergievski, A.P., 2009. Geological position and composition of Au–Ag ores of Central Chukotka. RUDN J. Eng. Res., No. 1, 48–52.

Nikolaev, Yu.N., Prokof'ev, V.Yu., Apletalin, A.V., Vlasov, E.A., Baksheev, I.A., Kal'ko, I.A., Komarova, Ya.S., 2013. Gold–telluride mineralization of the western Chukchi Peninsula, Russia: mineralogy, geochemistry, and formation conditions. Geol. Ore Deposits 55 (2), 96–124, doi: 10.1134/S1075701513020049.

Nikolaev, Yu.N., Baksheev, I.A., Prokofiev, V.Yu., Nagornaya, E.V., Marushchenko, L.I., Sidorina, Yu.N., Chitalin, A.F., Kal'ko, I.A., 2016. Gold–silver mineralization in porphyry–epithermal systems of the Baimka trend, western Chukchi Peninsula, Russia. Geol. Ore Deposits 58 (4), 284–307, doi: 10.1134/S107570151604005X.

Nikolaev, Yu.N., Kal'ko, I.A., Baksheev, I.A., Apletalin, A.V., Vlasov, E.A., Khabibullina, Yu.N., Dzhedzheya, G.T., Prokof'ev, V.Yu., Tikhomirov, P.L., 2020. Gold–silver mineralization of the Oloi zone and its commercial prospects. Otechestvennaya Geologiya, No. 1, 45–58.

Petrov, S.F., Mikhailov, V.N., 1999. New mineral types of gold mineralization in volcanic strata of the Chukchi Peninsula, in: Integrated Studies of the Chukchi Peninsula (Problems of Geology and Biogeography) [in Russian]. ChF SVKNII SVNTs RAN, Magadan, pp. 31–48.

Pingitore, N.E., Ponce, B.F., Eastman, M.P., Moreno, F., Podpora, C., 1992. Solid solutions in the system Ag_2S–Ag_2Se. J. Mater. Res. 7, 2219–2224, doi: 10.1557/JMR.1992.2219.

Pingitore, N.E., Ponce, B.F., Estrada, L., Eastman, M.P., Yuan, H.L., Porter, L.C., Estrada, G., 1993. Calorimetric analysis of the system Ag_2S–Ag_2Se between 25 and 250 ºC. J. Mater. Res. 8, 3126–3130, doi: 10.1557/JMR.1993.3126.

Prokofiev, V.Yu., Volkov, A.V., Kalko, I.A., Nikolayev, Yu.N., Sidorov, A.A., Vlasov, E.A., Wolfson, A.A., Sidorova, N.V., 2019a. Conditions of formation of Ag–Au epithermal mineralization in the Uteveyem ore cluster (Central Chukotka). Bulletin of the North-East Scientific Center of FEB RAS, No. 3, 19–26.

Prokofiev, V.Yu., Volkov, A.V., Nikolaev, Yu.N., Kal'ko, I.A., Vlasov, E.A., Vol'fson, A.A., Sidorov, A.A., 2019b. Formation conditions of epithermal Au–Ag mineralization of the Kaienmyvaam ore field (Central Chukchi region). Rudy i Metally, No. 1, 52–57.

Richards, J.P., 2013. Giant ore deposits formed by optimal alignments and combinations of geological processes. Nat. Geosci. 6, 911–916, doi: 10.1038/ngeo1920.

Roedder, E., 1984. Fluid Inclusions. Reviews in Mineralogy. Mineralogical Society of America, Washington.

Sakhno, V.G., Tsurikova, L.S., Maksimov, S.O., 2019. Geochronological and geochemical features of magmatic gold- and silverbearing complexes in the Chukotka sector of the Russian Arctic coast. Lithosphere (Russia) 19 (6), 861–888.

Savva, N.E., 2005. The probable source of selenium at volcanic deposits, in: The Science of Northeastern Russia at the Beginning of the New Century. Proceedings of the All-Russian Scientific Memorial Conference Dedicated to the 70th Birthday Anniversary of Academician K.V. Simakov, Magadan, 26–28 April 2005 [in Russian]. SVNTs DVO RAN, Magadan, pp. 208–210.

Savva, N.E., 2018. Mineralogy of Silver in Northeastern Russia [in Russian]. Triumf, Moscow.

Savva, N.E., Pal'yanova, G.A., Byankin, M.A., 2012. The problem of genesis of gold and silver sulfides and selenides in the Kupol deposit (Chukotka, Russia). Russ. Geol. Geophys. 53 (5), 457–466, doi: 10.1016/j.rgg.2012.03.006.

Savva, N.E., Kolova, E.E., Fomina, M.I., Kurashko, V.V., Volkov, A.V., 2016. Gold–base metallic mineralization in explosive breccias: mineral and genetic aspects (Sentyabr'skoe SV deposit, Chukotka). Bulletin of the North-East Scientific Center of FEB RAS, No. 1, 16–36.

Savva, N.E., Volkov, A.V., Sidorov, A.A., Byankin, M.A., 2021. The relationship among the orebody, volcanic rocks, and a rhyolite dike at the epithermal Kupol deposit (Western Chukotka). J. Volcanol. Seismol. 15 (3), 169–179, doi: 10.1134/S0742046321030052.

Shikazono, N., Nakata, M., Shimizu, M., 1990. Geochemical, mineralogic and geologic characteristics of Se- and Te-bearing epithermal gold deposits in Japan. Min. Geol. 40 (5), 337–352.

Shpikerman, V.I., 1998. Pre-Cretaceous Minerageny of Northeastern Asia [in Russian]. SVKNII DVO RAN, Magadan.

Sidorov, A.A., 1966. Gold–Silver Mineralization of the Central Chukchi Peninsula [in Russian]. Nauka, Moscow.

Sidorov, A.A., Vashchilov, Yu.Ya., Volkov, A.V., Belyi, V.F., 2008. Deep structure of the Kayemraveem ore district (Chukotka) and features of epithermal gold–silver mineralization. Dokl. Earth Sci. 421 (1), 755–759, doi: 10.1134/s1028334x08050097.

Sidorov, A.A., Belyi, V.F., Volkov, A.V., Savva, N.E., Alekseev, V. Yu., Kolova, E.E., 2009. The gold–silver Okhotsk–Chukotka volcanic belt. Geol. Ore Deposits 51 (6), 441–455, doi: 10.1134/s1075701509060026.

Simmons, S.F., White, N.C., John, D.A., 2005. Geological characteristics of epithermal precious and base metal deposits, in: Economic Geology 100th Anniversary Volume. Society of Economic Geologists, Littleton, CO, pp. 485–522.

Sokolov, S.D., Bondarenko, G.E., Morozov, O.L., Grigor'ev, V.N., 1999. The Asian continent–Northwest Pacific transition zone in the Late Jurassic–Early Cretaceous, in: Theoretical and Regional Problems of Geodynamics [in Russian]. Nauka, Moscow, pp. 30–84.

Sokolov, S.D., Tuchkova, M.I., Ledneva, G.V., Luchitskaya, M.V., Ganelin, A.V., Vatrushkina, E.V., Moiseev, A.V., 2021. Tectonic position of the South Anyui suture. Geotectonics 55 (5), 697–716, doi: 10.1134/S0016852121050083.

Thomson, B., Téllez, C., Dietrich, A., Oliver, N.H.S., Akinin, V., Blenkinsop, T.G., Guskov, A., Benowitz, J., Layer, P.W., Polzunenkov, G., 2021. The Dvoinoye and September Northeast high-grade epithermal Au–Ag veins, Vodorazdelnaya district, Chukotka region, Russia. Miner. Deposita, https://doi.org/10.1007/s00126-021-01065-0.

Tikhomirov, P.L., Kalinina, E.A., Moriguti, T., Makishima, A., Kobayashi, K., Cherepanova, I.Yu., Nakamura, E., 2012. The Cretaceous Okhotsk–Chukotka Volcanic Belt (NE Russia): geology, geochronology, magma output rates, and implications on the genesis of silicic LIPs. J. Volcanol. Geotherm. Res. 221–222, 14–32, doi: 10.1016/j.jvolgeores.2011.12.011.

Tikhomirov, P.L., Prokof'ev, V.Yu., Kal'ko, I.A., Apletalin, A.V., Nikolaev, Yu.N., Kobayashi, K., Nakamura, E., 2017. Post-collisional magmatism of western Chukotka and Early Cretaceous tectonic rearrangement in Northeastern Asia. Geotectonics 51 (2), 131–151, doi: 10.1134/S0016852117020054.

Umitbaev, R.B., 1986. The Okhotsk–Chaun Metallogenic Province [in Russian]. Nauka, Moscow.

Vartanyan, S.S., Lorents, D.A., Sergievskii, A.P., Shchepot'ev, Yu.M., 2005. Gold–silver ores of the Kaiemraveem cluster of the Chukchi Autonomous District. Otechestvennaya Geologiya, No. 4, 10–16.

Vlasov, E.A., Prokof'ev, V.Yu., Nikolaev, Yu.N., Kal'ko, I.A., 2016. New finding of gold–telluride mineralization on the Chukchi Peninsula: mineralogy and formation conditions of the Televeem ore occurrence. Rudy i Metally, No. 4, 48–59.

Volkov, A.V., Prokof'ev, V.Yu., 2011. Formation conditions and composition of ore-forming fluids in the Promezhutochnoe gold and silver deposit (Central Chukchi Peninsula, Russia). Russ. Geol. Geophys. 52 (11), 1448–1460, doi: 10.1016/j.rgg.2011.10.013.

Volkov, A.V., Goncharov, V.I., Sidorov, A.A., 2006. Gold and Silver Deposits of the Chukchi Peninsula [in Russian]. SVKNII DVO RAN, Magadan.

Volkov, A.V., Prokof'ev, V.Yu., Savva, N.E., Sidorov, A.A., Byankin, M.A., Uyutnov, K.V., Kolova, E.E., 2012. Ore formation at the Kupol epithermal gold–silver deposit in Northeastern Russia deduced from fluid inclusion study. Geol. Ore Deposits 54 (4), 295–303, doi: 10.1134/S107570151204006X.

Volkov, A.V., Savva, N.E., Kolova, E.E., Prokofiev, V.Yu., Murashov, K.Yu., 2018. Dvoinoe Au–Ag epithermal deposit, Chukchi Peninsula, Russia. Geol. Ore Deposits 60 (6), 527–545, doi: 10.1134/S1075701518060053.

Volkov, A.V., Prokofiev, V.Yu., Sidorov, A.A., Vinokurov, S.F., Elmanov, A.A., Murashov, K.Yu., Sidorova, N.V., 2019. The conditions of generation for the Au–Ag epithermal mineralization in the Amguema–Kanchalan volcanic field, Eastern Chukotka. J. Volcanol. Seismol. 13 (5), 335–347, doi: 10.1134/S0742046319050063.

Volkov, A.V., Prokof'ev, V.Yu., Vinokurov, S.F., Andreeva, O.V., Kiseleva, G.D., Galyamov, A.L., Murashov, K.Yu., Sidorova, N.V., 2020. Valunistoe epithermal Au–Ag deposit (East Chukotka, Russia): geological structure, mineralogical–geochemical peculiarities and mineralization conditions. Geol. Ore Deposits 62 (2), 97–121, doi: 10.1134/S1075701520020075.

White, N.C., Hedenquist, J.W., 1995. Epithermal gold deposits: Styles, characteristics and exploration. SEG Newslett. 23, 9–13.

Zhuravkova, T.V., Palyanova, G.A., Kravtsova, R.G., 2015. Physicochemical formation conditions of silver sulfoselenides at the Rogovik Deposit, northeastern Russia. Geol. Ore Deposits 57 (4), 313–330, doi: 10.1134/S1075701515040066.

Zhuravkova, T.V., Palyanova, G.A., Kalinin, Yu.A., Goryachev, N.A., Zinina, V.Yu., Zhitova, L.M., 2019. Physicochemical conditions of formation of gold and silver parageneses at the Valunistoe deposit (Chukchi Peninsula). Russ. Geol. Geophys. 60 (11), 1247–1256, doi: 10.15372/RGG2019118.